IEEE Access
Multidisciplinary | Rapid Review | Open Access Journal

Received March 7, 2021, accepted March 30, 2021, date of publication April 5, 2021, date of current version April 13, 2021.

Digital Object Identifier 10.1109/ACCESS.2021.3070921

Optimal Bit Allocation-Based Hybrid Precoder-Combiner Design Techniques for mmWave MIMO-OFDM Systems

MANJEER MAJUMDER, (Student Member, IEEE), HARSHIT SAXENA, SURAJ SRIVASTAVA, (Graduate Student Member, IEEE), AND ADITYA K. JAGANNATHAM, (Member, IEEE)

Department of Electrical Engineering, Indian Institute of Technology Kanpur, Kanpur 208016, India

Corresponding author: Manjeer Majumder (manjeer@iitk.ac.in)

This work was supported in part by the Science and Engineering Research Board (SERB), Department of Science and Technology, Government of India, in part by the Space Technology Cell, IIT Kanpur, in part by the IIMA IDEA Telecom Centre of Excellence, in part by the Qualcomm Innovation Fellowship, and in part by the Arun Kumar Chair Professorship.

ABSTRACT This work conceives techniques for the design of hybrid precoders/combiners for optimal bit allocation in frequency selective millimeter wave (mmWave) multiple-input multiple-output (MIMO) orthogonal frequency division multiplexing (OFDM) systems, toward transmission rate maximization. Initially, the optimal fully digital ideal precoder/ combiner design is derived together with a closed-form expression for the optimal bit allocation in the above system. This is followed by the development of a framework for optimal transceiver design and bit allocation in a practical mmWave MIMO-OFDM implementation with a hybrid architecture. It is demonstrated that the pertinent problem can be formulated as a multiple measurement vector (MMV)-based sparse signal recovery problem for joint design of the RF and baseband components across all the subcarriers, and an explicit algorithm is derived to solve this using the simultaneous orthogonal matching pursuit (SOMP). To overcome the shortcomings of the SOMP-based greedy approach, an MMV sparse Bayesian learning (MSBL)-based state-of-the-art algorithm is subsequently developed, which is seen to lead to improved performance due to the superior sparse recovery properties of the Bayesian learning framework. Simulation results verify the efficacy of the proposed designs and also demonstrate that the performance of the hybrid transceiver is close to that of its fully-digital counterpart.

INDEX TERMS Millimeter wave, frequency selective, MIMO, OFDM, hybrid precoder/ combiner, optimal bit allocation, sparse Bayesian learning, simultaneous orthogonal matching pursuit.

I. INTRODUCTION

Millimeter-wave (mmWave) wireless communication has attracted significant attention due to the availability of vast spectral bands that can in turn enable ultra-high data rates in 5G networks [1]–[3]. This has heralded a new epoch in the development of wireless communication technology, and cellular systems. However, mmWave bands suffer from much higher propagation losses [4]–[6] when compared to conventional sub-6 GHz systems in the lower frequency bands. Recent research demonstrates that large antenna arrays at both the transmitter and receiver ends i.e., multiple-input-multiple-output (MIMO) techniques, rendered possible due to the very small wavelengths, can provide significant beamforming gain [7]–[9] to successfully overcome the high propagation losses. Also, since mmWave systems, most likely, operate on wideband channels with a large bandwidth, orthogonal frequency division multiplexing (OFDM) coupled with MIMO has been acknowledged as a promising technology to overcome the inter-symbol interference (ISI) arising due to the frequency selective nature of the channel [10]–[12]. Furthermore, in the mmWave MIMO regime, the traditional transceiver design, based on a fully-digital implementation of the precoder and combiner, is highly

The associate editor coordinating the review of this manuscript and approving it for publication was Irfan Ahmed.

infeasible as it necessitates a dedicated radio frequency (RF) chain, DAC/ ADC for each antenna element [13], [14]. This arises due to the increased cost, area, and complexity of RF components operating in the mmWave regime, coupled with the high power consumption of the ADCs that are required to operate at a very high sampling rate. This has led to massive research in alternative signal processing paradigms for efficient implementation of mmWave MIMO communication. Recently, hybrid architectures that spread the signal processing operations over the analog and digital domains, have gained much popularity as they warrant a substantially lower number of RF chains. Such a hybrid beamformer can achieve a very high spectral efficiency, while simultaneously limiting the power consumption in comparison to the traditional MIMO architecture [15]–[19]. The RF precoder and combiner in such a system are implemented via constant magnitude analog phase shifters to compensate for the large scale path loss and shadowing effects at mmWave bands, while the digital precoder and combiner can provide the necessary flexibility to perform spatial multiplexing using only a very small number of RF chains. A brief review of the various works in the existing literature on the design of hybrid signal processing techniques for mmWave MIMO systems is presented next.

A. RELATED WORKS

A major fraction of the prior works have been devoted to investigate hybrid precoding and combing algorithms in narrowband mmWave channels [14], [20], [21]. Extensions to wideband hybrid precoder and combiner designs have been explored in [5], [12], [22]. Authors in [5] study the feasibility of attaining gigabit-per-second data rates for distances up to 1 km using millimeter-wave mobile broadband (MMB) links in an urban environment. In [22], Kim *et al.* present and thoroughly study a multi-beam diversity scheme for single-stream transmission in MIMO-OFDM systems. In [23], the authors proposed an iterative hybrid beamformer algorithm to maximize the average spectral efficiency in mmWave MIMO-OFDM systems with the aid of classical block coordination descent technique. The authors in [24] explored the hybrid beamforming optimization problem for mmWave MIMO-OFDM systems considering beam squint effect. In a radically different approach [14], [21], [25], [26] exploit the sparse scattering characteristic of mmWave MIMO channels for hybrid transceiver design, and the associated analog beamformers are chosen from predetermined dictionaries, such as the array response vectors over an angular grid or the well-known discrete Fourier transform (DFT) matrix. An innovative and practically appealing scheme for hybrid beamforming with single-stream transmission in MIMO-OFDM systems was discussed in [22], which employs an exhaustive search over the RF and baseband codebooks. However, no specific criterion was suggested for the design of the pertinent codebooks. As an improvement over the earlier approach, the authors in [12] derived a scheme for the optimal design of the baseband precoders by employing a predefined RF codebook.

Coming next to the signal processing strategies that can be employed in such systems, recent research has also shown that sparse signal recovery algorithms are eminently suited for mmWave MIMO systems due to the sparse characteristic of multi-path signal transmission. In order to leverage this important characteristic feature of such systems, reference [14] conceives an orthogonal matching pursuit (OMP)-based approach, which exhibits an excellent improvement in performance over traditional approaches. Authors in [27] present a novel iterative technique based on the OMP algorithm for designing the hybrid precoder. For ease of practical implementation, [28] proffers a transceiver design that has a much lower complexity. The authors in reference [29], [30] propose a codebook-based joint hybrid transceiver formulation considering the transmission of multiple streams in mmWave MIMO systems. The work in [14], develops an equivalent multiple measurement vector (MMV) problem for sparse signal reconstruction for optimal transmit precoder and receive combiner design, which was subsequently solved employing the greedy simultaneous orthogonal matching pursuit (SOMP) technique. Further, the SOMP technique is a greedy algorithm and its performance is sensitive to the selection of the dictionary matrix and stopping condition. These aspects often lead to convergence errors and poor performance of the precoder combiner thus determined. The sparse Bayesian learning (SBL) technique, described in the seminal work in [31], offers an excellent alternative to avoid this obstacle. The SBL algorithm determines the sparsest representation of the digital precoding/combining transceiver, characterized by the array response vectors, owing to the fact that the global minimum of the SBL cost function is attained at the sparsest solution. Moreover, the SBL algorithm converges to a fixed point of the log-likelihood cost function due to the advantage offered by the EM algorithm, thus ensuring robust performance with limited complexity, independent of the choice of initialization. Its performance guarantees coupled with ease of implementation make it perfectly applicable for the design of the precoder and combiner in mmWave MIMO-OFDM systems.

Various optimization criteria have been successfully explored for optimal transceiver design in conventional MIMO systems. In [32], the authors developed an optimal transceiver design for MIMO single carrier and multi carrier block transmission systems that minimizes the weighted combination of symbol estimation errors under the transmit power constraint. The optimal transceiver for OFDM systems described in [33] has been formulated to minimize the uncoded bit error rate (BER) with a unitary constraint imposed upon the precoder. The work in [34] develops an optimal transceiver filterbank structure for redundant block transmission system for two different formulations, viz., maximizing the output signal to noise ratio (SNR) under the zero-forcing (ZF) constraint and minimizing the mean squared error (MSE) subject to a total transmit

TABLE 1. A comparative visual summary of the contributions of existing papers on wideband frequency selective mmWave hybrid MIMO systems.

	[14]	[42]	[43]	[7]	[27]	[20]	[2]	[44]	[45]	[18]	[19]	[35]	[41]	[24]	[23]	**Proposed**
mmWave MIMO system	✓	✓	✓	✓	✓	✓	✓	✓	✓	✓	✓	×	×	✓	✓	✓
Frequency-flat channel	✓	×	×	×	×	×	✓	✓	×	✓	✓	✓	✓	×	×	×
Frequency-selective channel	×	✓	✓	✓	✓	✓	×	×	✓	×	×	×	×	✓	✓	✓
Optimal bit allocation	×	×	×	×	×	×	×	×	×	×	×	✓	✓	×	×	✓
OFDM	×	×	✓	✓	×	×	×	×	✓	×	×	×	×	✓	✓	✓
Dynamic QAM-modulation	×	×	×	✓	×	×	×	×	×	×	×	✓	✓	×	×	✓
SOMP	×	×	×	×	✓	✓	✓	×	×	×	×	×	×	×	×	✓
MSBL	×	×	×	×	×	×	×	×	×	×	×	×	×	×	×	✓
Hybrid precoder design	✓	✓	✓	✓	✓	✓	✓	✓	✓	✓	✓	×	×	✓	✓	✓
Hybrid combiner design	✓	✓	✓	×	✓	✓	✓	✓	×	✓	✓	×	×	×	✓	✓

power constraint. The authors in [35] developed an optimal MIMO transceiver that minimizes the uncoded BER subject to both individual and total power constraints using principles of convex optimization and majorization theory. The work detailed in reference [36] designs the MIMO transceiver by minimizing the MSE and BER under the total as well as peak transmit power constraints. A minimum BER design with a channel independent transmitter is derived in [37]. A ZF solution that minimizes the total transmit power for a given BER is developed in [38]. In [39], [40], Palomar *et al.* designed the optimal MIMO transceiver under an exhaustive set of quality of service (QoS) constraints such as MSE, signal to interference noise ratio (SINR), BER, further explored the problem of symbol constellation optimization. Vaidyanathan *et al.* described a novel approach in [41] for joint transceiver optimization and bit allocation toward transmission rate maximization. To the best of our knowledge, as can also be seen from the table above, none of the existing works have considered the problem of hybrid precoder/combiner design with optimal bit allocation for mmWave MIMO-OFDM systems toward bit-rate maximization, which therefore forms the focus of this work. For ease of reading, a quick comparative visual summary of the various contributions of the salient works reviewed above is given in Table 1. The contributions of this work are listed below.

B. CONTRIBUTIONS OF THIS WORK

A brief itemized description of the novel contributions of this work follows.

- This work considers hybrid precoder and combiner design for a single user wideband frequency selective spatially sparse mmWave MIMO-OFDM system. We begin with developing a procedure for joint design of the digital precoder and combiner by considering the zero forcing (ZF) design principle, which significantly lowers the signal processing complexity at the receiver. In addition, the proposed design maximizes the transmission rate by attaining the optimal bit allocation. An important aspect of the proposed design is that the optimal fully digital transceiver and the bit allocation are obtained in a closed form.
- This framework is subsequently extended to mmWave MIMO-OFDM implementation with a hybrid precoding/ combining transceiver, in which the analog precoder and combiner are constrained to have constant magnitude elements. Owing to the sparse multi-path scattering in a typical mmWave MIMO system, the resulting channel is spatially sparse. This useful property is exploited to develop a simplistic procedure for hybrid transceiver design by employing the multicarrier Simultaneous Orthogonal Matching Pursuit (SOMP) technique. The beam squint effect has also been considered in the SER performance of the proposed MSBL scheme to demonstrate its performance in a practical wideband channel.
- Furthermore, the SOMP algorithm, although efficient and yields acceptable performance, is often plagued by issues related to convergence due to its sensitivity to the choice of the dictionary matrix. To overcome this, a multicarrier transceiver design is presented for mmWave MIMO-OFDM systems, based on the state-of-the-art Multiple Sparse Bayesian Learning (M-SBL) algorithm for simultaneous sparse signal recovery. This is seen to achieve a better performance in comparison to the SOMP scheme in terms of improved symbol error rate (SER) and reduced number of RF chains.
- Subsequently, an integer bit allocation algorithm that assigns bits in an optimal fashion across input symbol streams of each subcarrier is developed to maximize the bit rate as well as to enhance the power efficacy.
- Exhaustive simulation results demonstrate the improved transmission rate performance of the proposed designs and also that the performance of the proposed hybrid precoder combiner is close to that of its ideal fully digital counterpart. This is significant since it evidences the fact that one can achieve a performance close to the ideal system with a only fraction of the number of RF chains, thus significantly lowering the power consumption and cost of hardware implementation.

The organization of the paper and notation are described next.

C. ORGANIZATION

The rest of the paper is organized as follows: Section II introduces the mmWave MIMO-OFDM system and channel model followed by formulation of the optimization problem for bit-rate maximization. Section III determines the ideal

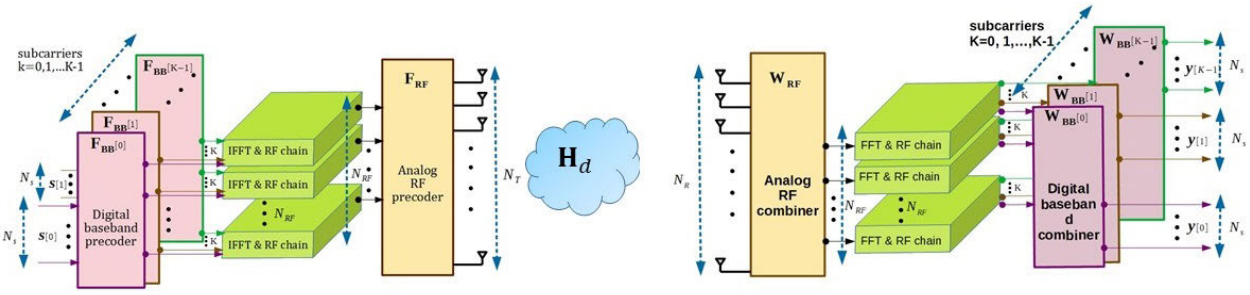

FIGURE 1. The hybrid precoding and combining transceiver architecture for a typical mmWave MIMO-OFDM system.

fully-digital precoder/combiner designs with the QoS constraint pertaining to the symbol error rate (SER) and total transmit power. Section IV develops the design of a practical hybrid transceiver for a mmWave MIMO-OFDM system followed by SOMP-based greedy approach. Section V then describes an equivalent MSBL algorithm for improved hybrid precoder/combiner design in the above system followed by a discussion on optimal bit allocation. The performance of the proposed scheme is validated via the simulation results presented in section VI followed by our overall assessment and concluding remarks in section VII. For reading convenience, the proofs of some of the propositions have been moved to the appendices at the end of the paper.

Notation: The following notation is employed across this paper. The operators $(\cdot)^T$, $(\cdot)^*$ and $(\cdot)^H$, denote the transpose, conjugate and Hermitian of a matrix, respectively. $\mathbb{C}^{M\times N}$ is the set of $M\times N$ matrices comprising of complex entries. $\mathbb{E}\{\cdot\}$ represents the statistical expectation operator. $\mathbf{I}_N$ denotes an $N\times N$ identity matrix. $|\cdot|$, $\|\cdot\|$, $\|\cdot\|_F$ and $\|\cdot\|_0$ denote the scalar magnitude, vector norm, matrix Frobenius norm and l_0-norm respectively. $\mathbf{M}(i,:)$ and $\mathbf{M}(:,j)$ denote the ith row and jth column of a matrix $\mathbf{M}$ respectively. The standard Gaussian $\mathbf{Q}$ function, defined as $\mathbf{Q}(x)=\frac{1}{\sqrt{2\pi}}\int_x^\infty e^{-y^2/2}dy$ is denoted by $\mathbf{Q}(x)$.

II. mmWave MIMO-OFDM SYSTEM MODEL AND PROBLEM FORMULATION

Consider an OFDM based mmWave hybrid MIMO system, as described in [13], [14], [45], with N_T transmit antennas, N_R receive antennas and N_{RF} RF chains, where $N_{\mathrm{RF}} \leq \min(N_R, N_T)$ at the transmitter as well as at the receiver. Consider $N_s \leq N_{\mathrm{RF}}$ parallel input symbol streams for K subcarriers in the mmWave MIMO-OFDM system. A block diagram of the mmWave hybrid MIMO-OFDM systems is shown in Fig. 1. Here, $\mathbf{F}_{\mathrm{BB}}[k] \in \mathbb{C}^{N_{\mathrm{RF}}\times N_s}$ represents the frequency-selective baseband precoder for the kth subcarrier and $\mathbf{F}_{\mathrm{RF}} \in \mathbb{C}^{N_T\times N_{\mathrm{RF}}}$ denotes the frequency-flat analog domain RF precoder. Thus, the frequency-selective hybrid precoder $\mathbf{F}[k] \in \mathbb{C}^{N_T\times N_s}$ corresponding to the kth subcarrier is given as $\mathbf{F}[k] = \mathbf{F}_{\mathrm{RF}}\mathbf{F}_{\mathrm{BB}}[k]$. Similarly, at the receiver, $\mathbf{W}_{\mathrm{BB}}[k] \in \mathbb{C}^{N_{\mathrm{RF}}\times N_s}$ represents the frequency-selective baseband combiner corresponding to the kth subcarrier, whereas $\mathbf{W}_{\mathrm{RF}} \in \mathbb{C}^{N_R\times N_{\mathrm{RF}}}$ denotes the analog domain RF combiner, which is frequency-flat. Hence, the hybrid combiner $\mathbf{W}[k] \in \mathbb{C}^{N_R\times N_s}$ at the receiver is given as $\mathbf{W}[k] = \mathbf{W}_{\mathrm{RF}}\mathbf{W}_{\mathrm{BB}}[k]$. Employing the hybrid precoder and combiner, as described above, the received signal $\mathbf{y}[k] \in \mathbb{C}^{N_s\times 1}$ at the output of the baseband combiner is expressed as

$$\mathbf{y}[k] = \mathbf{W}_{\mathrm{BB}}^H[k]\mathbf{W}_{\mathrm{RF}}^H\mathbf{H}[k]\mathbf{F}_{\mathrm{RF}}\mathbf{F}_{\mathrm{BB}}[k]\mathbf{s}[k] + \mathbf{W}_{\mathrm{BB}}^H[k]\mathbf{W}_{\mathrm{RF}}^H\mathbf{n}[k], \quad (1)$$

where $\mathbf{s}[k] \in \mathbb{C}^{N_s\times 1}$ denotes the baseband quadrature amplitude modulated (QAM) symbol vector and $\mathbf{n}[k] \sim \mathcal{CN}\left(\mathbf{0}, \sigma_n^2\mathbf{I}_{N_R}\right)$ represents additive white Gaussian noise (AWGN). Furthermore, the symbols of the vector $\mathbf{s}[k]$ are assumed to be uncorrelated with zero mean, and thus, the covariance matrix $\Lambda_s[k] = \mathbb{E}\left\{\mathbf{s}[k]\mathbf{s}^H[k]\right\}$ is diagonal with elements $[\Lambda_s[k]]_{i,i} = \sigma_{s_{i,k}}^2$, $i = 0, 1, \ldots, N_s-1$ on its principal diagonal. The quantity $\mathbf{H}[k] \in \mathbb{C}^{N_R\times N_T}$ represents the mmWave MIMO-OFDM channel matrix corresponding to the kth subcarrier. It is important to note that the RF precoder $\mathbf{F}_{\mathrm{RF}}$ and combiner $\mathbf{W}_{\mathrm{RF}}$ are implemented using analog phase-shifters, whose phase elements are digitally controlled, while amplitudes are constant. Thus, their elements are restricted as $\left|[\mathbf{F}_{\mathrm{RF}}]_{i,j}\right| = \frac{1}{\sqrt{N_T}}$ and $\left|[\mathbf{W}_{\mathrm{RF}}]_{i,j}\right| = \frac{1}{\sqrt{N_R}}$, $\forall\, i, j$, without loss of generality. The next subsection describes the wideband fequency-selective mmWave MIMO-OFDM channel model.

A. mmWave MIMO-OFDM CHANNEL MODEL

The dth delay tap of the wideband mmWave MIMO channel, denoted as $\mathbf{H}_d \in \mathbb{C}^{N_R\times N_T}$, $d = 0, 1, \ldots, N_c-1$, can be expressed as [42], [45]

$$\mathbf{H}_d = \sqrt{\frac{N_T N_R}{L}}\sum_{l=1}^{L}\alpha_l p_{rc}(dTs-\tau_l)\mathbf{a}_R(\theta_l^R)\mathbf{a}_T^H(\theta_l^T), \quad (2)$$

where α_l, θ_l^R and θ_l^T represent the complex path gain, angle of arrival (AoA) and angle of departure (AoD), respectively, associated with the lth spatial multipath component of the mmWave MIMO channel, and L denotes the number of multipath components. The quantity, $p_{rc}(\cdot)$ represents the combination of pulse-shaping and other low pass filters, T_s represents the sampling period and τ_l denotes the delay corresponding

to the lth multipath component. The vectors $\mathbf{a}_R(\theta_l^R) \in \mathbb{C}^{N_R \times 1}$ and $\mathbf{a}_T(\theta_l^T) \in \mathbb{C}^{N_T \times 1}$ denote the receive and transmit uniform linear array (ULA) response vectors respectively [9], [13], corresponding to the lth multipath, and are expressed as

$$\mathbf{a}_R(\theta_l^R) = \frac{1}{\sqrt{N_R}}\left[1, e^{-j\frac{2\pi}{\lambda}d_R\cos(\theta_l^R)}, \ldots, e^{-j\frac{2\pi}{\lambda}(N_R-1)d_R\cos(\theta_l^R)}\right]^T, \tag{3}$$

$$\mathbf{a}_T(\theta_l^T) = \frac{1}{\sqrt{N_T}}\left[1, e^{-j\frac{2\pi}{\lambda}d_T\cos(\theta_l^T)}, \ldots, e^{-j\frac{2\pi}{\lambda}(N_T-1)d_T\cos(\theta_l^T)}\right]^T, \tag{4}$$

where λ represents the wavelength of the transmitted signal, d_R and d_T stand for the inter-antenna spacings at the receiver and at the transmitter ends, respectively. ULAs have been chosen for the proposed wideband mmWave MIMO system owing to their higher RF processing speed, lower complexity feeding circuits and substantially lower inter-element coupling losses [46], [47]. The mmWave MIMO channel tap $\mathbf{H}_d$ described in (2) can be succinctly expressed as

$$\mathbf{H}_d = \mathbf{A}_R(\theta_R)\mathbf{D}_d\mathbf{A}_T^H(\theta_T), \tag{5}$$

where the matrices $\mathbf{A}_R(\theta_R) \in \mathbb{C}^{N_R \times L}$ and $\mathbf{A}_T(\theta_T) \in \mathbb{C}^{N_T \times L}$ denote the transmit and receive array response matrices described as

$$\mathbf{A}_R(\theta_R) = \left[\mathbf{a}_R\left(\theta_1^R\right), \mathbf{a}_R\left(\theta_2^R\right), \ldots, \mathbf{a}_R\left(\theta_L^R\right)\right], \tag{6}$$

$$\mathbf{A}_T(\theta_T) = \left[\mathbf{a}_T\left(\theta_1^T\right), \mathbf{a}_T\left(\theta_2^T\right), \ldots, \mathbf{a}_T\left(\theta_L^T\right)\right]. \tag{7}$$

The quantity $\mathbf{D}_d$ denotes a diagonal matrix of size $L \times L$ with the diagonal elements being the complex path gains $\{\alpha_l p_{rc}(dTs - \tau_l)\}_{l=1}^L$. Finally, the frequency-domain representation of the mmWave MIMO-OFDM channel matrix $\mathbf{H}[k]$ corresponding to kth subcarrier is expressed as

$$\mathbf{H}[k] = \sum_{d=0}^{N_c-1}\mathbf{H}_d\exp\left(\frac{-j2\pi kd}{K}\right) = \mathbf{A}_R(\theta_R)\mathbf{D}[k]\mathbf{A}_T^H(\theta_T), \tag{8}$$

where $\mathbf{D}[k] \in \mathbb{C}^{L\times L}$ is once again a diagonal matrix that obeys $\mathbf{D}[k] = \sum_{d=0}^{N_c-1}\mathbf{D}_d\exp\left(-j\frac{2\pi kd}{K}\right)$. The next section describes the design of the optimal fully-digital precoder and combiner for mmWave hybrid MIMO-OFDM systems.

B. PROBLEM FORMULATION

The key aim of this subsection is to jointly develop a design of the hybrid ZF transceiver and optimally allocate input bits to maximize the number of bits transmitted per block with a given symbol error rate (SER) constraint for the mmWave MIMO-OFDM system. The transmitted signal $\mathbf{x}[k] \in \mathbb{C}^{N_T\times 1}$ at the kth subcarrier is given as $\mathbf{x}[k] = \mathbf{F}_{\mathrm{RF}}\mathbf{F}_{\mathrm{BB}}[k]\mathbf{s}[k] \in \mathbb{C}^{N_T\times 1}$, whose transmit power is expressed as

$$\mathbb{E}\left\{\mathbf{x}^H[k]\mathbf{x}[k]\right\} = \mathrm{Tr}\left(\mathbf{F}_{\mathrm{RF}}\mathbf{F}_{\mathrm{BB}}[k]\mathbf{\Lambda}_s[k]\mathbf{F}_{\mathrm{BB}}^H[k]\mathbf{F}_{\mathrm{RF}}^H\right). \tag{9}$$

The combined noise vector $\widetilde{\mathbf{n}}[k] \in \mathbb{C}^{N_s\times 1}$ at the kth subcarrier obeys $\widetilde{\mathbf{n}}[k] = \mathbf{W}_{\mathrm{BB}}^H[k]\mathbf{W}_{\mathrm{RF}}^H\mathbf{n}[k]$. Thus, the power of each element of the combined noise $\widetilde{\mathbf{n}}[k]$, denoted by $\sigma_{n_{i,k}}^2$, is given as

$$\sigma_{n_{i,k}}^2 = \sigma_n^2\left[\mathbf{W}_{\mathrm{BB}}^H[k]\mathbf{W}_{\mathrm{RF}}^H\mathbf{W}_{\mathrm{RF}}\mathbf{W}_{\mathrm{BB}}[k]\right]_{i,i}. \tag{10}$$

Let SER denote the target QoS and $b_{i,k}$ denote the number of bits carried by the ith symbol stream at the kth subcarrier. For the QAM modulated symbol vector $\mathbf{s}[k]$, one can express $b_{i,k}$ as

$$b_{i,k} = \log_2\left(1 + \frac{\sigma_{s_{i,k}}^2}{\sigma_{n_{i,k}}^2\Gamma}\right), \tag{11}$$

where the quantity Γ obeys $\Gamma = \frac{1}{3}[\mathbf{Q}^{-1}(\mathrm{SER}/4)]^2$ [48]. Furthermore, for sufficiently high bit rate, i.e, $2^{b_{i,k}} \gg 1$, the expression for $b_{i,k}$ can be approximated as

$$b_{i,k} \approx \log_2\left(\frac{\sigma_{s_{i,k}}^2}{\sigma_{n_{i,k}}^2\Gamma}\right). \tag{12}$$

Using the above result, the objective function for bit-rate maximization in mmWave MIMO-OFDM transceiver design can be formulated as

$$\max_{\mathbf{W}[k],\mathbf{F}[k],\sigma_{s_{i,k}}^2}\sum_{k=0}^{K-1}\sum_{i=0}^{N_s-1}\left\lfloor\log_2\left(\frac{\sigma_{s_{i,k}}^2}{\sigma_{n_{i,k}}^2\Gamma}\right)\right\rfloor.$$

However, one can readily observe that this cost function is non-convex in nature, which renders it intractable. Therefore, this work follows a two-step procedure based on the standard integer relaxation approach [49]–[52] to simplify the design. The first step solves the optimization problem without considering the floor operation, followed by assigning the integer bits appropriately to the input symbol streams loaded over the sub-carriers, as described later in Algorithm 3. Therefore, the bit-rate maximization problem for mmWave MIMO-OFDM transceiver design can be formulated as

$$\max_{\mathbf{W}_{\mathrm{BB}}[k],\mathbf{W}_{\mathrm{RF}},\mathbf{F}_{\mathrm{BB}}[k],\mathbf{F}_{\mathrm{RF}},\sigma_{s_{i,k}}^2} b = \sum_{k=0}^{K-1}\sum_{i=0}^{N_s-1}\log_2\left(\frac{\sigma_{s_{i,k}}^2}{\sigma_{n_{i,k}}^2\Gamma}\right),$$

$$\text{s.t.}\begin{cases}\sum_{k=0}^{K-1}\mathrm{Tr}\left(\mathbf{F}_{\mathrm{RF}}\mathbf{F}_{\mathrm{BB}}[k]\Lambda_{\mathbf{s}}[k]\mathbf{F}_{\mathrm{BB}}^H[k]\mathbf{F}_{\mathrm{RF}}^H\right)\\ \le P_0,\\ \mathbf{W}_{\mathrm{BB}}^H[k]\mathbf{W}_{\mathrm{RF}}^H\mathbf{H}[k]\mathbf{F}_{\mathrm{RF}}\mathbf{F}_{\mathrm{BB}}[k] = \mathbf{I}_{N_s},\\ \sigma_{s_{i,k}}^2 \ge 0;\ k = 0, 1, \ldots, K-1;\\ i = 0, 1, \ldots, N_s - 1.\\ \left|[\mathbf{F}_{\mathrm{RF}}]_{i,j}\right| = \frac{1}{\sqrt{N_T}}\ \text{and}\ \left|[\mathbf{W}_{\mathrm{RF}}]_{i,j}\right|\\ = \frac{1}{\sqrt{N_R}}, \forall\, i, j,\end{cases} \tag{13}$$

where P_0 denotes the total transmit power. The first constraint limits the total transmit power, the second one represents the ZF condition for transceiver design, whereas the last constraint represents the constant magnitude restriction on the elements of the RF precoder and combiner. Furthermore, the ZF constraint simplifies the signal processing complexity significantly at the receiver, since the received signal

$\mathbf{y}[k]$ simply becomes the estimate of the transmitted signal $\mathbf{s}[k]$. It can be readily observed that the last constraint is non-convex in nature, which makes the overall optimization problem non-convex and intractable. However, by substituting $\mathbf{F}_{\mathrm{RF}}\mathbf{F}_{\mathrm{BB}}[k] = \mathbf{F}[k]$ and $\mathbf{W}_{\mathrm{RF}}\mathbf{W}_{\mathrm{BB}}[k] = \mathbf{W}[k]$, i.e., with the equivalent digital precoder and combiner, one can recast the above problem as the convex problem

$$\max_{\mathbf{W}[k],\mathbf{F}[k],\sigma^2_{s_{i,k}}} b = \sum_{k=0}^{K-1}\sum_{i=0}^{N_s-1}\log_2\left(\frac{\sigma^2_{s_{i,k}}}{\sigma^2_{n_{i,k}}\Gamma}\right),$$
$$\text{s.t.}\begin{cases}\sum_{k=0}^{K-1}\mathrm{Tr}\left(\mathbf{F}[k]\Lambda_{\mathbf{s}}[k]\mathbf{F}^H[k]\right)\le P_0,\\ \mathbf{W}^H[k]\mathbf{H}[k]\mathbf{F}[k]=\mathbf{I}_{N_s},\\ \sigma^2_{s_{i,k}}\ge 0;\ k=0,1,\ldots,K-1;\\ i=0,1,\ldots,N_s-1.\end{cases} \tag{14}$$

The optimal fully-digital precoder $\mathbf{F}[k]$ and combiner $\mathbf{W}[k]$ designs are described in the next section, followed by the hybrid precoder and combiner designs in the subsequent section.

III. OPTIMAL FULLY-DIGITAL PRECODER/WWWWW/COMBINER DESIGN WITH A QUALITY OF SERIVCE (QoS) CONSTRAINT

The optimization problem above is solved in two steps. The first step determines the optimal power allocation, i.e., $\sigma^2_{s_{i,k}}$ for each input symbol stream i and subcarrier k that maximizes the bit rate for a given precoder $\mathbf{F}[k]$ and combiner $\mathbf{W}[k]$. This is subsequently employed in the next step for the design of the optimal fully-digital precoder and combiner.

In order to derive the optimal power allocation, the Lagrangian for the optimization problem in Eq. (14) can be formulated as

$$\mathcal{L}\left(\alpha,\left\{\sigma^2_{s_{i,k}},\beta_{i,k}\right\}_{i=0,k=0}^{N_s-1,K-1}\right)$$
$$=\sum_{k=0}^{K-1}\sum_{i=0}^{N_s-1}\log_2\left(\frac{\sigma^2_{s_{i,k}}}{\sigma^2_{n_{i,k}}\Gamma}\right)+\alpha\sum_{k=0}^{K-1}\mathrm{Tr}\left(\mathbf{F}[k]\Lambda_s[k]\mathbf{F}^H[k]\right)$$
$$-\sum_{k=0}^{K-1}\sum_{i=0}^{N_s-1}\beta_{i,k}\sigma^2_{s_{i,k}}, \tag{15}$$

where α and $\beta_{i,k}$ are the Lagrange multipliers. Upon employing the Karush-Kuhn-Tucker (KKT) conditions, as described in Appendix-A, the optimal $\sigma^2_{s_{i,k}}$ is expressed as

$$\sigma^{2*}_{s_{i,k}} = \frac{P_0}{KN_s\left[\mathbf{F}^H[k]\mathbf{F}[k]\right]_{i,i}}. \tag{16}$$

Now, substituting Eq. (73) in the optimization objective, one can reformulate the bit rate expression as

$$b=\sum_{k=0}^{K-1}\sum_{i=0}^{N_s-1}\log_2\left(\frac{P_o}{KN_s\Gamma\left[\mathbf{F}^H[k]\mathbf{F}[k]\right]_{i,i}\sigma^2_{n_{i,k}}}\right)$$
$$=\log_2\left(\prod_{k=0}^{K-1}\prod_{i=0}^{N_s-1}\frac{P_o}{KN_s\Gamma\left[\mathbf{F}^H[k]\mathbf{F}[k]\right]_{i,i}\sigma^2_{n_{i,k}}}\right). \tag{17}$$

The design of optimal fully-digital ZF transceiver that maximizes the bit rate above is described next. Let the singular value decomposition (SVD) of the mmWave MIMO-OFDM channel matrix $\mathbf{H}[k]$ be given as

$$\mathbf{H}[k]=\mathbf{U}[k]\begin{bmatrix}\Lambda[k] & \mathbf{0}\\ \mathbf{0} & \mathbf{0}\end{bmatrix}\mathbf{V}^H[k], \tag{18}$$

where $\mathbf{U}[k]\in\mathbb{C}^{N_R\times N_R}$ and $\mathbf{V}[k]\in\mathbb{C}^{N_T\times N_T}$ denote the left and right singular matrices, which are unitary, and $\Lambda[k]\in\mathbb{R}^{\rho\times\rho}$ represents a diagonal matrix with non-zero singular values of $\mathbf{H}[k]$ on its principal diagonal. The quantity $\rho=\mathrm{rank}\,(\mathbf{H}[k])$, where $\rho\ge N_s$ for the ZF transceiver to exist. Lemma-1 and 2 described below have been employed for the design of the optimal precoder and combiner matrices.

Lemma 1: Without loss of generality, one can express the fully-digital precoder $\mathbf{F}[k]$ *in the following form*:

$$\mathbf{F}[k]=\mathbf{V}[k]\begin{bmatrix}\mathbf{A}[k]\\ \mathbf{0}\end{bmatrix}, \tag{19}$$

where $\mathbf{A}[k]\in\mathbb{C}^{\rho\times N_s}$ *and* $\mathrm{rank}(\mathbf{A}[k])=\rho$.

Proof: Proof is given in Appendix-C. □

Note that the hybrid precoder design requires channel state information at the transmitter (CSIT) in order to derive the optimal fully-digital precoder $\mathbf{F}[k]$ [1], [14], [53]. However, in practical scenarios, the CSI is estimated at the receiver and fed back to the transmitter using a limited feedback link. Designing the hybrid precoder using limited/ imperfect CSIT is a challenging problem, which may be considered as a possible future work.

Lemma 2: Without loss of generality, one can choose the fully-digital combiner $\mathbf{W}^H[k]$ *as*

$$\mathbf{W}^H[k]=(\mathbf{H}[k]\mathbf{F}[k])^\dagger$$
$$=\left(\mathbf{A}^H[k]\Lambda^2[k]\mathbf{A}[k]\right)^{-1}\left[\mathbf{A}^H[k]\Lambda[k]\ \mathbf{0}\right]\mathbf{U}^H[k], \tag{20}$$

where $\mathbf{A}[k]$ *is given in Eq.* (19).

Proof: Proof is given in Appendix-D □

Employing Lemma-2, the noise variance $\sigma^2_{n_{i,k}}$ is given as

$$\sigma^2_{n_{i,k}}=\sigma^2_n\left[\mathbf{W}^H[k]\mathbf{W}[k]\right]_{i,i}$$
$$=\sigma^2_n\left[\left(A^H[k]\Lambda^2[k]A[k]\right)^{-1}\right]_{i,i}. \tag{21}$$

Next, substituting the expression of $\mathbf{F}[k]$ from Lemma-1 and the quantity $\sigma^2_{n_{i,k}}$ from the above result, the bit rate b in Eq. (17) can be rewritten as

$$b=\log_2\left[\left(\frac{P_0}{KN_s\sigma^2_n\Gamma}\right)^{KN_s}\prod_{k=0}^{K-1}\prod_{i=0}^{N_s-1}\frac{\left[\mathbf{A}^H[k]\Lambda^2[k]\mathbf{A}[k]\right]_{i,i}}{\left[\mathbf{A}^H[k]\mathbf{A}[k]\right]_{i,i}}\right]. \tag{22}$$

From the above, one can readily observe that maximizing the bit rate b with respect to $\mathbf{A}[k]$ is equivalent to minimizing

$$\prod_{i=0}^{N_s-1}\frac{\left[\mathbf{A}^H[k]\mathbf{A}[k]\right]_{i,i}}{\left[\mathbf{A}^H[k]\Lambda^2[k]\mathbf{A}[k]\right]_{i,i}}. \tag{23}$$

Employing the Hadamard inequality [54], one can now lower bound the quantity in (23) as

$$\prod_{i=0}^{N_s-1} \frac{\left[\mathbf{A}^H[k]\mathbf{A}[k]\right]_{i,i}}{\left[\mathbf{A}^H[k]\Lambda^2[k]\mathbf{A}[k]\right]_{i,i}} \geq \frac{\det\left(\mathbf{A}^H[k]\mathbf{A}[k]\right)}{\det\left(\mathbf{A}^H[k]\Lambda^2[k]\mathbf{A}[k]\right)}. \tag{24}$$

Furthermore, equality in Eq. (24) holds only if the following two conditions are satisfied: (i) $\mathbf{A}^H[k]\mathbf{A}[k]$ is a diagonal matrix, (ii) $\mathbf{A}^H[k]\Lambda^2[k]\mathbf{A}[k]$ is a diagonal matrix. This in turn implies that the columns of both $\mathbf{A}[k]$ and $\mathbf{A}[k]\Lambda[k]$ have to be orthogonal. Therefore, the matrix $\mathbf{A}[k]\Lambda[k]$ can be expressed as

$$\begin{aligned} &\mathbf{A}[k]\Lambda[k] = \mathbf{Q}[k]\mathbf{D}[k] \\ \implies &\mathbf{A}[k] = \Lambda^{-1}[k]\mathbf{Q}[k]\mathbf{D}[k], \end{aligned} \tag{25}$$

where $\mathbf{Q}^H[k]\mathbf{Q}[k] = \mathbf{I}_{N_s}$, i.e. $\mathbf{Q}[k]$ denotes a $\rho \times N_s$ semi-unitary matrix and $\mathbf{D}[k]$ represents an $N_s \times N_s$ diagonal matrix with non-zero diagonal entries. Using Eq. (25) we can write

$$\frac{\det\left(\mathbf{A}^H[k]\mathbf{A}[k]\right)}{\det\left(\mathbf{A}^H[k]\Lambda^2[k]\mathbf{A}[k]\right)} = \frac{1}{\det\left(\mathbf{Q}^H[k]\Lambda^{-2}[k]\mathbf{Q}[k]\right)}. \tag{26}$$

Since, the above result is independent of the diagonal matrix $\mathbf{D}[k]$, one can choose $\mathbf{D}[k] = \mathbf{I}_{N_s}$, without loss of generality. Therefore, the bit rate in Eq. (22) can be modified as

$$b = \log_2\left[\left(\frac{P_0}{KN_s\sigma_n^2\Gamma}\right)^{KN_s} \prod_{k=0}^{K-1} \frac{1}{\det\left(\mathbf{Q}^H[k]\Lambda^{-2}[k]\mathbf{Q}[k]\right)}\right]. \tag{27}$$

Hence, in order to design the optimal fully-digital precoder and combiner, one only needs to focus on finding the matrix $\mathbf{Q}[k]$ that minimizes $\det\left(\mathbf{Q}^H[k]\Lambda^{-2}[k]\mathbf{Q}[k]\right)$, which can be obtained by employing the Poincaré separation theorem [54], as described below.

Theorem 1 (Poincaré Separation Theorem): Consider an $n \times n$ Hermitian matrix $\mathbf{B}$ and an $n \times r$ semi-unitary matrix $\mathbf{C}$, where $\mathbf{C}^H\mathbf{C} = \mathbf{I}_r$. It then follows that

$$\lambda_i(\mathbf{B}) \leq \lambda_i\left(\mathbf{C}^H\mathbf{B}\mathbf{C}\right) \leq \lambda_{n-r+i}(\mathbf{B}),\ i = 0, 1, \ldots, r-1, \tag{28}$$

where $\lambda_i(\mathbf{Y})$ represents the ith smallest eigenvalue of the matrix $\mathbf{Y}$.

Proof: Proof is given in [54]. □

Since the diagonal elements of the matrix $\Lambda[k]$ are arranged in decreasing order, employing the above theorem, one can write

$$\left[\Lambda^{-2}[k]\right]_{i,i} \leq \lambda_i\left(\mathbf{Q}^H[k]\Lambda^{-2}[k]\mathbf{Q}[k]\right), \quad i = 0, 1, \ldots, N_s-1. \tag{29}$$

Furthermore, the matrix $\Lambda^{-2}[k]$ is a positive definite matrix, which implies $\left[\Lambda^{-2}[k]\right]_{i,i} > 0,\ i = 0, 1, \ldots, N_s-1$. Therefore,

$$\begin{aligned} &\prod_{i=0}^{N_s-1} \lambda_i\left(\mathbf{Q}^H[k]\Lambda^{-2}[k]\mathbf{Q}[k]\right) \geq \prod_{i=0}^{N_s-1}\left[\Lambda^{-2}[k]\right]_{i,i} \\ \implies &\det\left(\mathbf{Q}^H[k]\Lambda^{-2}[k]\mathbf{Q}[k]\right) \geq \det\left(\Lambda_{N_s}^{-2}[k]\right), \end{aligned} \tag{30}$$

where the matrix $\Lambda_{N_s}[k]$ denotes an $N_s \times N_s$ diagonal matrix whose diagonal entries are the N_s dominant singular values of the mmWave MIMO-OFDM channel matrix $\mathbf{H}[k]$. It can be readily observed that equality in (30) holds if the matrix $\mathbf{Q}[k]$ obeys $\mathbf{Q}[k] = \begin{bmatrix}\mathbf{I}_{N_s} & \mathbf{0}_{N_s\times(\rho-N_s)}\end{bmatrix}^T$. Thus, one can obtain the optimal matrix $\mathbf{A}[k]$, which minimizes (23), and in turn, maximizes (17), as

$$\mathbf{A}[k] = \Lambda^{-1}[k]\mathbf{Q}[k]\mathbf{D}[k] = \begin{bmatrix}\Lambda_{N_s}^{-1}[k] \\ \mathbf{0}\end{bmatrix}. \tag{31}$$

Employing the above key result, the optimal fully-digital precoder $\mathbf{F}[k]$ and combiner $\mathbf{W}[k]$ for the kth subcarrier can be derived using Lemma-1 and 2 as follows:

$$\mathbf{F}[k] = \mathbf{V}[k]\begin{bmatrix}\Lambda_{N_s}^{-1}[k] \\ \mathbf{0}\end{bmatrix}, \quad \mathbf{W}[k] = \mathbf{U}[k]\begin{bmatrix}\mathbf{I}_{N_s} \\ \mathbf{0}\end{bmatrix}. \tag{32}$$

The optimization problem in Eq. (14) can also be solved without taking the approximation in Eq. (12) to derive the bit allocation given by $b_{i,k}^{\text{new}}$, as shown in Appendix-B, and also reproduced below:

$$\begin{aligned} b_{i,k}^{\text{new}} = \log_2\Bigg(&\frac{P_0}{KN_s\Gamma\left[\mathbf{F}^H[k]\mathbf{F}[k]\right]_{i,i}\sigma_{n_{i,k}}^2} \\ &+ \frac{\sum_{k=0}^{K-1}\sum_{i=0}^{N_s-1}\left[\mathbf{F}^H[k]\mathbf{F}[k]\right]_{i,i}}{KN_s\left[\mathbf{F}^H[k]\mathbf{F}[k]\right]_{i,i}}\Bigg). \end{aligned} \tag{33}$$

However, the expression for $b_{i,k}^{\text{new}}$ renders the optimization problem for hybrid transceiver design intractable. Thus, the high bit-rate approximation of Eq. (12) is essentially employed to obtain closed form expressions of the fully-digital precoder and combiner, whereas the optimal integer bit allocation procedure developed in Algorithm-3 employs the exact bit-rate expression, thus emphasizing the practical suitability of the design procedure. Moreover, it can be readily observed that at high SNR, $b_{i,k}^{\text{new}} \longrightarrow b_{i,k}$, which is identical to the solution obtained with the high-bit rate assumption.

IV. HYBRID PRECODER/WWWWW/COMBINER DESIGN FOR mmWave MIMO OFDM SYSTEMS

This section develops hybrid precoder and combiner designs for mmWave MIMO-OFDM systems. We begin by describing the design of the hybrid precoder. The problem for design of the baseband precoder $\mathbf{F}_{\text{BB}}[k]$ and the RF precoder $\mathbf{F}_{\text{RF}}$ can be formulated as

$$\begin{aligned} &\left(\left\{\mathbf{F}_{\text{BB}}^*[k]\right\}_{k=0}^{K-1}, \mathbf{F}_{\text{RF}}^*\right) \\ &= \arg\min_{\{\mathbf{F}_{\text{BB}}[k]\}_{k=0}^{K-1}, \mathbf{F}_{\text{RF}}} \sum_{k=0}^{K-1} \|\mathbf{F}[k] - \mathbf{F}_{\text{RF}}\mathbf{F}_{\text{BB}}[k]\|_F^2 \end{aligned}$$

$$\text{s.t. } \left|[\mathbf{F}_{\text{RF}}]_{i,j}\right| = \frac{1}{\sqrt{N_T}}, \quad \forall\, i,j. \tag{34}$$

Concatenating the optimal digital precoders $\mathbf{F}[k]$ obtained from (32) and the baseband precoders $\mathbf{F}_{\text{BB}}[k]$ across all the K subcarriers as

$$\mathbf{F} = \left[\mathbf{F}[0], \mathbf{F}[1], \ldots \mathbf{F}[K-1]\right] \in \mathbb{C}^{N_T \times KN_s}, \tag{35}$$

$$\mathbf{F}_{\text{BB}} = \left[\mathbf{F}_{\text{BB}}[0], \mathbf{F}_{\text{BB}}[1], \ldots \mathbf{F}_{\text{BB}}[K-1] \in \mathbb{C}^{N_{\text{RF}} \times KN_s}\right], \tag{36}$$

and noting the fact that the RF precoder $\mathbf{F}_{\text{RF}}$ is frequency-flat, one can recast Eq. (32) as

$$\left(\mathbf{F}^*_{\text{BB}}, \mathbf{F}^*_{\text{RF}}\right) = \arg \min_{\mathbf{F}_{\text{BB}}, \mathbf{F}_{\text{RF}}} \|\mathbf{F} - \mathbf{F}_{\text{RF}}\mathbf{F}_{\text{BB}}\|_F^2 \quad \text{s.t. } \left|[\mathbf{F}_{\text{RF}}]_{i,j}\right| = \frac{1}{\sqrt{N_T}}, \quad \forall\, i,j. \tag{37}$$

One can now employ the following key observations to simplify the hybrid precoder design procedure. As derived in (8), the mmWave MIMO-OFDM channel matrix $\mathbf{H}[k]$ corresponding to the kth subcarrier can be expressed as $\mathbf{H}[k] = \mathbf{A}_R(\theta_R)\mathbf{D}[k]\mathbf{A}_T^H(\theta_T)$, which implies that the row and column spaces of $\mathbf{H}[k]$ are subsets of the column space of the transmit and receive array response matrices $\mathbf{A}_T(\theta_T)$ and $\mathbf{A}_R(\theta_R)$, respectively, i.e,

$$\mathcal{R}(\mathbf{H}[k]) \subseteq \mathcal{C}(\mathbf{A}^*_T(\theta_T)) \text{ and } \mathcal{C}(\mathbf{H}[k]) \subseteq \mathcal{C}(\mathbf{A}_R(\theta_R)), \tag{38}$$

where $\mathcal{R}(\cdot)$ and $\mathcal{C}(\cdot)$ represent the row and column spaces, respectively, of a matrix. Furthermore, from Eq. (32), it follows that

$$\mathcal{C}(\mathbf{F}[k]) \subseteq \mathcal{C}(\mathbf{V}[k]). \tag{39}$$

Finally, employing the SVD of the mmWave MIMO-OFDM channel matrix $\mathbf{H}[k]$ described in (18), together with (35), (38) and (39), one can conclude that

$$\mathcal{C}(\mathbf{F}) \subseteq \mathcal{C}(\mathbf{A}_T(\theta_T)). \tag{40}$$

Therefore, in order to simplify the hybrid precoder design, the columns of the RF precoder $\mathbf{F}_{\text{RF}}$ can be suitably selected from the columns of the transmit array response matrix $\mathbf{A}_T(\theta_T)$. Interestingly, this choice also satisfies the non-convex constraint in (37). Thus, the mmWave hybrid precoder design problem can be reformulated as follows. Let $\widetilde{\mathbf{F}}_{\text{BB}} \in \mathbb{C}^{L \times KN_s}$ denote an intermediate baseband precoding matrix, whose N_{RF} non-zero rows constitute the desired baseband precoder $\mathbf{F}_{\text{BB}}$. Then, we can recast (37) as

$$\arg \min_{\widetilde{\mathbf{F}}_{\text{BB}}} \left\|\mathbf{F} - \mathbf{A}_T(\theta_T)\widetilde{\mathbf{F}}_{\text{BB}}\right\|_F^2 \quad \text{s.t. } \left\|\text{diag}\left(\widetilde{\mathbf{F}}_{\text{BB}}\widetilde{\mathbf{F}}^H_{\text{BB}}\right)\right\|_0 = N_{\text{RF}}, \tag{41}$$

where the constraint (41) arises since only N_{RF} rows are allowed to be non-zero in the matrix $\widetilde{\mathbf{F}}_{\text{BB}}$. From the solution of the above optimization problem, which will be described in the next subsection and in Section-V, one can obtain the RF precoder $\mathbf{F}_{\text{RF}}$ by extracting the columns of $\mathbf{A}_T(\theta_T)$, whose indices correspond to those of the non-zero rows of $\widetilde{\mathbf{F}}_{\text{BB}}$.

In practical scenarios, where the true transmit array response matrix $\mathbf{A}_T(\theta_T)$ is unknown in (41), one can employ a transmit array response dictionary matrix constructed from a G_T-quantized angular-grid as described next. Let the set $\Theta_T = \left\{\theta_{1,T}, \theta_{2,T}, \ldots, \theta_{G_T,T}\right\}$ denote the quantized angular-grid spanning the AoD space. The transmit array response dictionary matrix $\mathbf{A}_{T,D}(\Theta_T) \in \mathbb{C}^{N_T \times G_T}$ is constructed as

$$\mathbf{A}_{T,D}(\Theta_T) = \left[\mathbf{a}_T\left(\theta_{1,T}\right), \mathbf{a}_T\left(\theta_{2,T}\right), \ldots, \mathbf{a}_T\left(\theta_{G_T,T}\right)\right]. \tag{42}$$

The equivalent hybrid precoder design problem for the mmWave MIMO-OFDM systems is given as

$$\arg \min_{\widetilde{\mathbf{F}}_{\text{BB},D}} \left\|\mathbf{F} - \mathbf{A}_{T,D}(\Theta_T)\widetilde{\mathbf{F}}_{\text{BB},D}\right\|_F^2 \quad \text{s.t. } \left\|\text{diag}\left(\widetilde{\mathbf{F}}_{\text{BB},D}\widetilde{\mathbf{F}}^H_{\text{BB},D}\right)\right\|_0 = N_{\text{RF}}, \tag{43}$$

where $\widetilde{\mathbf{F}}_{\text{BB},D} \in \mathbb{C}^{G_T \times KN_s}$ denotes the intermediate baseband precoder matrix corresponding to the transmit dictionary $\mathbf{A}_{T,D}(\theta_T)$. It is important to note that the matrix $\widetilde{\mathbf{F}}_{\text{BB},D}$, owing to the constraint in (43), can only have N_{RF} non-zero rows, which implies that it is block-sparse in nature. Also, the resulting optimization problem is popularly known as an MMV-based sparse signal recovery problem, and the techniques to solve this are described in the later part of this section.

Along similar lines, one can formulate the hybrid combiner design problem for a mmWave MIMO-OFDM system as

$$\arg \min_{\widetilde{\mathbf{W}}_{\text{BB},D}} \left\|\mathbf{W} - \mathbf{A}_{R,D}(\Theta_R)\widetilde{\mathbf{W}}_{\text{BB},D}\right\|_F^2 \quad \text{s.t. } \left\|\text{diag}\left(\widetilde{\mathbf{W}}_{\text{BB},D}\widetilde{\mathbf{W}}^H_{\text{BB},D}\right)\right\|_0 = N_{\text{RF}}, \tag{44}$$

where $\widetilde{\mathbf{W}}_{\text{BB},D} \in \mathbb{C}^{N_{\text{RF}} \times KN_s}$ denotes the intermediate baseband combiner, whereas the matrix $\mathbf{W} \in \mathbb{C}^{N_R \times KN_s}$ is the concatenated optimal digital combiner defined as

$$\mathbf{W} = [\mathbf{W}[0], \mathbf{W}[1], \ldots, \mathbf{W}[K-1]]. \tag{45}$$

The quantity $\mathbf{A}_{R,D}(\Theta_R) \in \mathbb{C}^{N_R \times G_R}$ represents the receive array response dictionary matrix constructed as

$$\mathbf{A}_{R,D}(\Theta_R) = \left[\mathbf{a}_R\left(\theta_{1,R}\right), \mathbf{a}_R\left(\theta_{2,R}\right), \ldots, \mathbf{a}_R\left(\theta_{G_R,R}\right)\right], \tag{46}$$

where the set $\Theta_R = \left\{\theta_{1,R}, \theta_{2,R}, \ldots, \theta_{G_R,R}\right\}$ denotes the quantized angular-grid spanning the AoA space. Note that the design problem in (44) is once again an MMV-based sparse signal recovery problem. Finally, the concatenated baseband combiner defined as $\mathbf{W}_{\text{BB}} = [\mathbf{W}_{\text{BB}}[0], \mathbf{W}_{\text{BB}}[1], \ldots, \mathbf{W}_{\text{BB}}[K-1]]$ can be extracted from the non-zero rows of the matrix $\widetilde{\mathbf{W}}_{\text{BB},D}$ and the RF combiner $\mathbf{W}_{\text{RF}}$ can be obtained by extracting the corresponding columns of the receive dictionary matrix $\mathbf{A}_{R,D}(\Theta_R)$. Algorithm 1 describes the proposed SOMP technique for designing the baseband precoder $\mathbf{F}_{\text{BB}}[k]$, $0 \le k \le K-1$, and the RF precoder $\mathbf{F}_{\text{RF}}$. The combiner design follows similarly.

Algorithm 1 Simultaneous Orthogonal Matching Pursuit (SOMP) Algorithm to Design Hybrid Precoder in mmWave MIMO-OFDM Systems

Required: Concatenated optimal fully-Digital precoder $\mathbf{F}$, transmit array response dictionary matrix $\mathbf{A}_{T,D}(\Theta_T)$, number of RF chains N_{RF}.

1) $\mathbf{F}_{\text{RF}} = [\,]$
2) $\mathbf{F}_{\text{res}} = \mathbf{F}$
3) **for** $i \leq N_{\text{RF}}$ **do**
4) $\quad \Psi = \mathbf{A}_{T,D}^{H}(\Theta_T)\mathbf{F}_{\text{res}}$
5) $\quad k = \arg\max_{l=1,2,\ldots,G} \left(\Psi\Psi^{H}\right)_{l,l}$
6) $\quad \mathbf{F}_{\text{RF}} = \left[\mathbf{F}_{\text{RF}} \mid \mathbf{A}_{T,D}(\Theta_T)(:,k)\right]$
7) $\quad \mathbf{F}_{\text{BB}} = \left(\mathbf{F}_{\text{RF}}^{H}\mathbf{F}_{\text{RF}}\right)^{-1}\mathbf{F}_{\text{RF}}^{H}\mathbf{F}$
8) $\quad \mathbf{F}_{\text{res}} = \mathbf{F} - \mathbf{F}_{\text{RF}}\mathbf{F}_{\text{BB}}$
9) **end for**
10) **Return** $\mathbf{F}_{\text{RF}}$, $\mathbf{F}_{\text{BB}}$

V. MSBL FOR HYBRID PRECODER/WWWWW/ COMBINER DESIGN IN mmWave MIMO-OFDM SYSTEMS

The proposed MSBL technique is a Bayesian method of sparse signal recovery, which assigns the parameterized Gaussian prior below to the ith row of the intermediate baseband precoder $\widetilde{\mathbf{F}}_{\text{BB},D}$ [31]

$$p\left(\widetilde{\mathbf{F}}_{\text{BB},D}(i,:);\zeta_i\right) = \mathcal{CN}\left(\mathbf{0},\zeta_i\mathbf{I}_{KN_s}\right) = \prod_{j=1}^{KN_s}(\pi\zeta_i)^{-1}\exp\left(-\frac{\left|\widetilde{\mathbf{F}}_{\text{BB},D}(i,j)\right|^2}{\zeta_i}\right). \tag{47}$$

From the prior assignment as seen above, it can be noted that the hyperparameter ζ_i, $1 \leq i \leq G_T$, parameterizes the covariance matrix of the multivariate prior associated with the ith row of the matrix $\widetilde{\mathbf{F}}_{\text{BB},D}$. Let $\boldsymbol{\mathcal{Z}} = \text{diag}\left(\zeta_1,\zeta_2,\ldots,\zeta_{G_T}\right) \in \mathbb{R}^{G_T\times G_T}$ represent the hyperparameter matrix. The prior assignment for the intermediate baseband precoder $\widetilde{\mathbf{F}}_{\text{BB},D}$ is given as

$$p\left(\widetilde{\mathbf{F}}_{\text{BB},D};\boldsymbol{\mathcal{Z}}\right) = \prod_{i=1}^{G_T} p\left(\widetilde{\mathbf{F}}_{\text{BB},D}(i,:);\zeta_i\right). \tag{48}$$

The MMSE estimate $\widehat{\mathbf{F}}_{\text{BB},D} \in \mathbb{C}^{G_T\times KN_s}$ of the intermediate baseband precoder $\widetilde{\mathbf{F}}_{\text{BB},D}$ can be determined as [55]

$$\widehat{\mathbf{F}}_{\text{BB},D} = \sigma_e^{-2}\Sigma\mathbf{A}_{T,D}^{H}(\Theta_T)\mathbf{F}, \tag{49}$$

where the associated error covariance matrix $\Sigma \in \mathbb{C}^{G_T\times G_T}$ is obtained as

$$\Sigma = \left(\sigma_e^{-2}\mathbf{A}_{T,D}^{H}(\Theta_T)\mathbf{A}_{T,D}(\Theta_T) + \boldsymbol{\mathcal{Z}}^{-1}\right)^{-1}. \tag{50}$$

The quantity σ_e^2 in the above expressions denotes the variance of each element of the approximation error $\left(\mathbf{F} - \mathbf{A}_{T,D}(\Theta_T)\widetilde{\mathbf{F}}_{\text{BB},D}\right)$. It can be readily observed that the MMSE estimate $\widehat{\mathbf{F}}_{\text{BB},D}$ in (49) depends on the hyperparameter matrix $\boldsymbol{\mathcal{Z}}$, through the associated error covariance matrix Σ. In addition, it can be observed from (47) that as the hyperparameter $\zeta_i \to 0$, the associated ith row of the intermediate baseband precoder $\widetilde{\mathbf{F}}_{\text{BB},D}(i,:) \to \mathbf{0}_{KN_s\times 1}$ [31]. Therefore, estimating the block-sparse matrix $\widetilde{\mathbf{F}}_{\text{BB},D}$ translates to estimating the corresponding hyperparameter matrix $\boldsymbol{\mathcal{Z}}$. For superior MMV-based sparse signal recovery, the proposed MSBL approach obtains the estimate $\widehat{\boldsymbol{\mathcal{Z}}}$, which maximizes the log-Bayesian evidence $\log\left[p(\mathbf{F};\boldsymbol{\mathcal{Z}})\right]$, evaluated as

$$\log\left[p(\mathbf{F};\boldsymbol{\mathcal{Z}})\right] = \kappa_1 - KN_s\log\left[\det\left(\boldsymbol{\Sigma}_F\right)\right] - \sum_{j=1}^{KN_s}\mathbf{F}(:,j)\boldsymbol{\Sigma}_F^{-1}\mathbf{F}^{H}(:,j), \tag{51}$$

where the quantity $\boldsymbol{\Sigma}_F = \sigma_e^2\mathbf{I}_{N_T} + \mathbf{A}_{T,D}(\Theta_T)\boldsymbol{\mathcal{Z}}\mathbf{A}_{T,D}^{H}(\Theta_T) \in \mathbb{C}^{N_T\times N_T}$ and the constant $\kappa_1 = -KN_s\log(\pi)$. As described in [31], the log-Bayesian evidence maximization above with respect to the hyperparameter matrix $\boldsymbol{\mathcal{Z}}$ has several maximas, which results in a non-concave problem. Thus, direct maximization of the log-Bayesian evidence for the estimation of $\boldsymbol{\mathcal{Z}}$ becomes infeasible. The well-known expectation-maximization (EM) [55], in such a scenario, is ideally suited for maximizing the cost function in each iteration, which guarantees convergence to a local optima. Therefore, the proposed MSBL-based framework employs the EM technique for estimation of the hyperparameters, and in turn, the block-sparse intermediate baseband precoder $\widetilde{\mathbf{F}}_{\text{BB},D}$. Furthermore, it has a geometric convergence rate as discussed in [56]. The key steps of the EM procedure are described next.

Let the complete information set be constructed as $\left\{\mathbf{F},\widetilde{\mathbf{F}}_{\text{BB},D}\right\}$. Let $\widehat{\boldsymbol{\mathcal{Z}}}^{(m-1)}$ denote the estimate of the hyperparameter matrix $\boldsymbol{\mathcal{Z}}$ in the $(m-1)$th iteration. The EM procedure to update the estimate $\widehat{\boldsymbol{\mathcal{Z}}}^{(m)}$ in the mth iteration is described below. It involves two steps, the expectation (E-step) and the maximization (M-step). In the E-step, the log-likelihood function $\mathcal{L}\left(\boldsymbol{\mathcal{Z}}|\widehat{\boldsymbol{\mathcal{Z}}}^{(m-1)}\right)$ of the complete information set is evaluated as

$$\begin{aligned}\mathcal{L}\left(\boldsymbol{\mathcal{Z}}|\widehat{\boldsymbol{\mathcal{Z}}}^{(m-1)}\right) &= \mathbb{E}_{\widetilde{\mathbf{F}}_{\text{BB},D}|\mathbf{F};\widehat{\boldsymbol{\mathcal{Z}}}^{(m-1)}}\left\{\log p\left(\mathbf{F},\widetilde{\mathbf{F}}_{\text{BB},D};\boldsymbol{\mathcal{Z}}\right)\right\}\\ &= \mathbb{E}\left\{\log\left[p\left(\mathbf{F}|\widetilde{\mathbf{F}}_{\text{BB},D}\right)\right] + \log\left[p\left(\widetilde{\mathbf{F}}_{\text{BB},D};\boldsymbol{\mathcal{Z}}\right)\right]\right\}.\end{aligned} \tag{52}$$

Subsequently, the maximization-step (M-step) maximizes $\mathcal{L}\left(\boldsymbol{\mathcal{Z}}|\widehat{\boldsymbol{\mathcal{Z}}}^{(m-1)}\right)$ with respect to the hyperparameter matrix $\boldsymbol{\mathcal{Z}}$. It can be readily observed that the first term $\mathbb{E}\left\{\log\left[p\left(\mathbf{F}|\widetilde{\mathbf{F}}_{\text{BB},D}\right)\right]\right\}$ in (52) can be simplified as

$$\mathbb{E}\left\{\log\left[p\left(\mathbf{F}|\widetilde{\mathbf{F}}_{\text{BB},D}\right)\right]\right\} = -N_TKN_s\log(\pi\sigma_e^2) - \sigma_e^{-2} \times \left\|\mathbf{F} - \mathbf{A}_{T,D}(\Theta_T)\widetilde{\mathbf{F}}_{\text{BB},D}\right\|_F^2, \tag{53}$$

which is independent of the hyperparameter matrix $\boldsymbol{\mathcal{Z}}$. Ignoring this term, the hyperparameter estimation in the M-step is equivalently expressed as

$$\widehat{\boldsymbol{\mathcal{Z}}}^{(m)} = \arg\max_{\boldsymbol{\mathcal{Z}}}\mathbb{E}\left\{\log\left[p\left(\widetilde{\mathbf{F}}_{\text{BB},D};\boldsymbol{\mathcal{Z}}\right)\right]\right\}. \tag{54}$$

Substituting $\log\left[p\left(\widetilde{\mathbf{F}}_{\mathrm{BB},D};\boldsymbol{\mathcal{Z}}\right)\right]$ from (48), the equivalent optimization problem for estimation of $\boldsymbol{\mathcal{Z}}$ is given as

$$\widehat{\boldsymbol{\mathcal{Z}}}^{(m)} \equiv \arg\max_{\boldsymbol{\mathcal{Z}}} \sum_{i=1}^{G_T} \Bigg[-KN_s \log(\zeta_i) - \frac{1}{\zeta_i} \sum_{j=1}^{KN_s} \mathbb{E}\left\{ \left| \widetilde{\mathbf{F}}_{\mathrm{BB},D}(i,j) \right|^2 \right\} \Bigg]. \quad (55)$$

It can be readily observed from (55) that the estimation of the hyperparameter matrix $\boldsymbol{\mathcal{Z}}$ is decoupled with respect to each hyperparameter ζ_i. Differentiating the objective function with respect to ζ_i and setting the resulting expression equal to zero yields the update $\widehat{\zeta}_i^{(m)}$ for the hyperparameter ζ_i, in the mth EM iteration, as

$$\widehat{\zeta}_i^{(m)} = \frac{1}{KN_s} \sum_{j=1}^{KN_s} \mathbb{E}_{\widetilde{\mathbf{F}}_{\mathrm{BB},D}|\mathbf{F};\widehat{\boldsymbol{\mathcal{Z}}}^{(m-1)}} \left\{ \left| \widetilde{\mathbf{F}}_{\mathrm{BB},D}(i,j) \right|^2 \right\}. \quad (56)$$

To evaluate the conditional expectation $\mathbb{E}_{\widetilde{\mathbf{F}}_{\mathrm{BB},D}|\mathbf{F};\widehat{\boldsymbol{\mathcal{Z}}}^{(m-1)}}\{\cdot\}$ for the above expression, the *a posteriori* probability density function (pdf) $p\left(\widetilde{\mathbf{F}}_{\mathrm{BB},D}|\mathbf{F};\widehat{\boldsymbol{\mathcal{Z}}}^{(m-1)}\right)$ of the intermediate baseband precoder $\widetilde{\mathbf{F}}_{\mathrm{BB},D}$ is evaluated as [55]

$$p\left(\widetilde{\mathbf{F}}_{\mathrm{BB},D}|\mathbf{F};\widehat{\boldsymbol{\mathcal{Z}}}^{(m-1)}\right) = \mathcal{CN}\left(\widehat{\mathbf{F}}_{\mathrm{BB},D}^{(m)}, \Sigma^{(m)}\right), \quad (57)$$

where the *a posteriori* mean $\widehat{\mathbf{F}}_{\mathrm{BB},D}^{(m)} \in \mathbb{C}^{G_T \times KN_s}$ and the associated covariance matrix $\Sigma^{(m)} \in \mathbb{C}^{G_T \times G_T}$ are obtained by setting $\boldsymbol{\mathcal{Z}} = \widehat{\boldsymbol{\mathcal{Z}}}^{(m-1)}$ in (49) and (50), respectively. Employing this *a posteriori* pdf, the quantity $\mathbb{E}\left\{ \left| \widetilde{\mathbf{F}}_{\mathrm{BB},D}(i,j) \right|^2 \right\}$ reduces to

$$\mathbb{E}\left\{ \left| \widetilde{\mathbf{F}}_{\mathrm{BB},D}(i,j) \right|^2 \right\} = \Sigma^{(m)}(i,i) + \left| \widehat{\mathbf{F}}_{\mathrm{BB},D}^{(m)}(i,j) \right|^2. \quad (58)$$

Substituting (58) into (56), the hyperparameter update is given as

$$\widehat{\zeta}_i^{(m)} = \Sigma^{(m)}(i,i) + \frac{1}{KN_s} \sum_{j=1}^{KN_s} \left| \widehat{\mathbf{F}}_{\mathrm{BB},D}^{(m)}(i,j) \right|^2. \quad (59)$$

The EM procedure described above are repeated for a maximum of $M_{\max}$ iterations or until $\left\| \widehat{\boldsymbol{\mathcal{Z}}}^{(m)} - \widehat{\boldsymbol{\mathcal{Z}}}^{(m-1)} \right\|_F^2 \leq \epsilon$, whichever is achieved earlier, where the stopping parameters ϵ and $M_{\max}$ are suitably chosen. As demonstrated in [31], the global minima of the MSBL-cost function guarantees the sparsest representation of $\mathbf{F}$ using the columns of the transmit array response dictionary matrix $\mathbf{A}_{T,D}(\Theta_T)$. Furthermore, by virtue of the EM algorithm, the convergence of the MSBL is guaranteed to a fixed point of the log-likelihood, from any initialization. The MSBL-based estimate $\widehat{\mathbf{F}}_{\mathrm{BB},D}^{\mathrm{MSBL}}$ of the intermediate baseband precoder is obtained as the converged *a-posteriori* mean $\widehat{\mathbf{F}}_{\mathrm{BB},D}^{(m)}$. Subsequently, the MSBL-based concatenated baseband precoder $\mathbf{F}_{\mathrm{BB}}^{\mathrm{MSBL}}$ for mmWave MIMO-OFDM systems can be extracted from $\widehat{\mathbf{F}}_{\mathrm{BB},D}^{\mathrm{MSBL}}$ using the procedure described next.

Let the ordered estimates of the hyperparameters be arranged as $\widehat{\zeta}_{k_1} \geq \widehat{\zeta}_{k_2} \geq \ldots \geq \widehat{\zeta}_{k_{G_T}}$. Let $\mathcal{K} = \{k_1, k_2, \ldots, k_{N_{\mathrm{RF}}}\}$ represent the set of indices of the N_{RF} hyperparameters having the largest magnitudes. The concatenated baseband precoder matrix $\mathbf{F}_{\mathrm{BB}}^{\mathrm{MSBL}}$ can be obtained from $\widehat{\mathbf{F}}_{\mathrm{BB},D}^{\mathrm{MSBL}}$ as

$$\mathbf{F}_{\mathrm{BB}}^{\mathrm{MSBL}} = \widehat{\mathbf{F}}_{\mathrm{BB},D}^{\mathrm{MSBL}}(\mathcal{K},:). \quad (60)$$

Similarly, the RF precoder $\mathbf{F}_{\mathrm{RF}}^{\mathrm{MSBL}}$ can be extracted from $\mathbf{A}_{T,D}(\Theta_T)$ by columns indexed by the set $\mathcal{K}$ as

$$\mathbf{F}_{\mathrm{RF}}^{\mathrm{MSBL}} = \mathbf{A}_{T,D}(\Theta_T)(:,\mathcal{K}). \quad (61)$$

A step-by-step procedure describing the MSBL-based hybrid precoder design is presented in Algorithm-2. A similar approach can also be leveraged to design the baseband and RF combiner $\mathbf{W}_{\mathrm{BB}}[k]$, $0 \leq k \leq K-1$, and $\mathbf{W}_{\mathrm{RF}}$, respectively, formulated in (44) for mmWave MIMO-OFDM systems. The hybrid precoder obtained from the MSBL-based design can now be employed for optimal bit allocation, as described in the next subsection.

Algorithm 2 MSBL Algorithm to Design Hybrid Precoder in mmWave MIMO-OFDM Systems

Input: Concatenated optimal fully-Digital precoder $\mathbf{F}$, transmit array response dictionary matrix $\mathbf{A}_{T,D}(\Theta_T)$, number of RF chains N_{RF}, variance of the approximation error σ_e^2, stopping parameters ϵ and $M_{\max}$

Initialization: $\widehat{\zeta}_i^{(0)} = 1,\ \forall\ 1 \leq i \leq G_T \rightarrow \widehat{\boldsymbol{\mathcal{Z}}}^{(0)} = \mathbf{I}_{G_T}$

Set counter $m = 0$ and $\widehat{\boldsymbol{\mathcal{Z}}}^{(-1)} = \mathbf{0}_{G_T \times G_T}$

while $\left(\left\| \widehat{\boldsymbol{\mathcal{Z}}}^{(m)} - \widehat{\boldsymbol{\mathcal{Z}}}^{(m-1)} \right\|_F^2 > \epsilon \text{ and } m < M_{\max} \right)$ **do**

$m \leftarrow m + 1$

E-step: Evaluate *a posteriori* covariance and mean

$$\Sigma^{(m)} = \left(\sigma_e^{-2} \mathbf{A}_{T,D}^H(\Theta_T) \mathbf{A}_{T,D}(\Theta_T) + \left(\widehat{\boldsymbol{\mathcal{Z}}}^{(m-1)} \right)^{-1} \right)^{-1}$$

$$\widehat{\mathbf{F}}_{\mathrm{BB},D}^{(m)} = \sigma_e^{-2} \Sigma^{(m)} \mathbf{A}_{T,D}^H(\Theta_T) \mathbf{F}$$

M-step: Evaluate hyperparameter estimates

for $i = 0, 1, \ldots, G_T$ **do**

$$\widehat{\zeta}_i^{(m)} = \Sigma^{(m)}(i,i) + \frac{1}{KN_s} \sum_{j=1}^{KN_s} \left| \widehat{\mathbf{F}}_{\mathrm{BB},D}^{(m)}(i,j) \right|^2$$

end for

end while

Set $\widehat{\mathbf{F}}_{\mathrm{BB},D}^{\mathrm{MSBL}} = \widehat{\mathbf{F}}_{\mathrm{BB},D}^{(m)}$

Output: Obtain $\mathbf{F}_{\mathrm{BB}}^{\mathrm{MSBL}}$ and $\mathbf{F}_{\mathrm{RF}}^{\mathrm{MSBL}}$ using (60) and (61), respectively

A. OPTIMAL BIT ALLOCATION FOR HYBRID PRECODER DESIGN IN mmWave MIMO-OFDM SYSTEMS

One of the key objectives of the proposed design is also to optimally allocate the number of bits $b_{i,k}$ to the ith input symbol stream at the kth subcarrier, such that the total number of

TABLE 2. Computational complexities of various steps in the *i*th iteration of the proposed SOMP algorithm.

Operation	Complex Multiplications (X)	Complex Additions (A)
Step - 4	$KG_T N_T N_s$	$KG_T N_s\,(N_T-1)$
Step - 7	$\frac{N_{\mathrm{RF}}^3}{2}+N_{\mathrm{RF}}^2\left(\frac{3}{2}+2N_T\right)+KN_{\mathrm{RF}}N_T N_s$	$\frac{N_{\mathrm{RF}}^3}{2}+N_{\mathrm{RF}}^2\left(N_T-\frac{3}{2}\right)+$ $N_{\mathrm{RF}}\left(KN_sN_T-N_T-KN_s\right)$
Step-8	$KN_{\mathrm{RF}}N_T N_s$	$KN_sN_T\,(N_{\mathrm{RF}}-1)$

Algorithm 3 Multicarrier Multistream Integer Bit Allocation in mmWave MIMO-OFDM Systems

Required: Hybrid combiner $\mathbf{F}_{\mathrm{RF}}^{\mathrm{MSBL}}$ and $\mathbf{F}_{\mathrm{BB}}^{\mathrm{MSBL}}[k]$ derived using MSBL, SER Γ, number of subcarriers K, number of input symbol streams N_s, total power P_0, noise power $\sigma_{n_{i,k}}^2$ after hybrid combining

Initialization: $\mathbf{F}^{\mathrm{M}}[k]=\mathbf{F}_{\mathrm{RF}}^{\mathrm{MSBL}}\mathbf{F}_{\mathrm{BB}}^{\mathrm{MSBL}}[k]$

1) **for** $k=0$ to $K-1$
2) Set $\widetilde{N}_s=N_s$
3) Calculate $g_{i,k}=\dfrac{P_0}{KN_s\sigma_{n_{i,k}}^2\Gamma\left[\left(\mathbf{F}^{\mathrm{M}}[k]\right)^H\left(\mathbf{F}^{\mathrm{M}}[k]\right)\right]_{i,i}}$, $\forall\, 0\le i\le\widetilde{N}_s-1$
4) **If** $g_{i,k}\ge 1,\ \forall\, 0\le i\le\widetilde{N}_s-1$, **go to** step-(5) **else** set $\widetilde{N}_s=\widetilde{N}_s-1$ and **go to** step-(3)
5) Calculate $b_{i,k}=\lfloor\log_2(1+g_{i,k})\rfloor,\ \forall\, 0\le i\le\widetilde{N}_s-1$
6) Assign $b_{i,k}=0,\ \forall\,\widetilde{N}_s\le i<N_s$
7) **end for**

bits allocated per block b, as described in (14), is maximized. To this end, employing the MSBL-based hybrid precoders $\mathbf{F}_{\mathrm{RF}}^{\mathrm{MSBL}}$ and $\mathbf{F}_{\mathrm{BB}}^{\mathrm{MSBL}}[k]$, together with (11) and (73), the number of bits $b_{i,k}$ can be obtained as

$$b_{i,k}=\log_2\left(1+\frac{P_0}{KN_s\sigma_{n_{i,k}}^2\Gamma\left[\left(\mathbf{F}^{\mathrm{M}}[k]\right)^H\left(\mathbf{F}^{\mathrm{M}}[k]\right)\right]_{i,i}}\right),\qquad(62)$$

where $\mathbf{F}^{\mathrm{M}}[k]=\mathbf{F}_{\mathrm{RF}}^{\mathrm{MSBL}}\mathbf{F}_{\mathrm{BB}}^{\mathrm{MSBL}}[k]$. It is noteworthy that the quantity $b_{i,k}$ might not always turn out to be an integer. A simple, yet inefficient, solution to deal with this problem is to use integer number of bits given by $\lfloor b_{i,k}\rfloor$, where $\lfloor\cdot\rfloor$ denotes the floor value. However, when

$$KN_s\sigma_{n_{i,k}}^2\Gamma\left[\left(\mathbf{F}^{\mathrm{M}}[k]\right)^H\left(\mathbf{F}^{\mathrm{M}}[k]\right)\right]_{i,i}\ge P_0,\qquad(63)$$

the quantity $\lfloor b_{i,k}\rfloor=0$. In such scenarios, the power $\sigma_{s_{i,k}}^2$ assigned to the ith input stream of the kth subcarrier is left unused. In order to tackle this power wastage during the bit allocation, one can implement the recursive bit allocation procedure described in Algorithm-3, which assigns the power only to those streams that correspond to the non-zero values of $\lfloor b_{i,k}\rfloor$.

B. COMPLEXITY ANALYSIS

This section presents a brief analysis of the computational complexities for the Algorithms 1, 2 and 3. As described in Table 1, the computational complexity of the proposed SOMP algorithm turns out to be $\mathcal{O}\left(KG_T N_T N_s\right)$, which arises from the computation of the matrix Ψ at each iteration. In Table 2, the computational cost of the proposed MSBL scheme is derived. It can be seen that the matrix inversion involved in calculating the matrix $\Sigma^{(m)}$ in the E-step results in the complexity of order $\mathcal{O}\left(G_T^3\right)$. Finally, the complexity of the integer bit allocation in Algorithm 3 turns out to be $\mathcal{O}\left(N_s^2 N_T\right)$.

VI. SIMULATION RESULTS

This section presents the simulation results to demonstrate the performance of the proposed multicarrier optimal bit allocation scheme for frequency selective mmWave MIMO-OFDM systems. The symbol error rate (SER) performance of the proposed multicarrier ZF transceiver is also illustrated for the same system. The transmission rate of the proposed multicarrier optimal bit allocation algorithm based on the fully-digital optimal precoder/ combiner is compared with that of the hybrid precoder/ combiner designs obtained using the multicarrier SOMP and MSBL approaches outlined in sections Algorithm 1 and V. The SER performance is also presented for the fully-digital, MSBL and SOMP based precoders/ combiners. Finally, the variation in the performance of multicarrier MSBL and SOMP algorithms for the hybrid precoder/ combiner design with the number of RF chains N_{RF} has also been demonstrated through simulation results. The following configurations are considered to comprehensively illustrate the performance for various systems. In System-I, the number of input symbol streams is set as $N_s=4$, number of transmit and receive antennas are $N_T=N_R=32$ and number of RF chains at the transmitter and receiver is set to $N_{\mathrm{RF}}=4$, whereas for System-II, the same are set as $N_s=8$ $N_T=N_R=64$, $N_{RF}=12$.

The wide band frequency-selective mmWave MIMO channel is assumed to be spatially sparse with the number of active paths set as $L=4$ and $L=8$ for System-I and System-II respectively, and the delay tap length is set to $N_c=4$ and $N_c=8$ for System-I and System-II respectively. The number of subcarriers for both the mmWave MIMO OFDM systems is fixed at $K=64$. The uniform linear arrays (ULAs) at the transmitter and the receiver have inter-antenna spacings fixed at $d_T=d_R=\dfrac{\lambda}{2}$. The uniform angular grid sizes for the set of feasible AoA/ AoDs space are set to $G=G_R=G_T=64$ and 128 for the 32×32 and 64×64 mmWave MIMO systems respectively. The signal to noise ratio (SNR) is defined as $\dfrac{P_0}{\sigma_n^2}$ and the noise vector

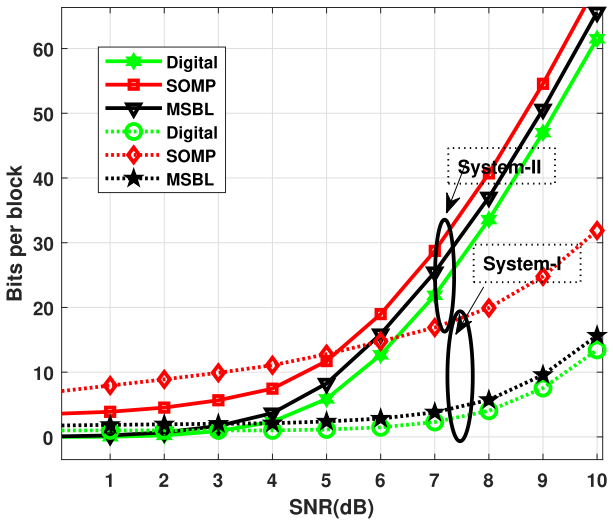

(a) Transmission bit rate vs SNR in dB at a fixed error rate $\Gamma = 10^{-5}$ for frequency selective mmWave MIMO systems I and II

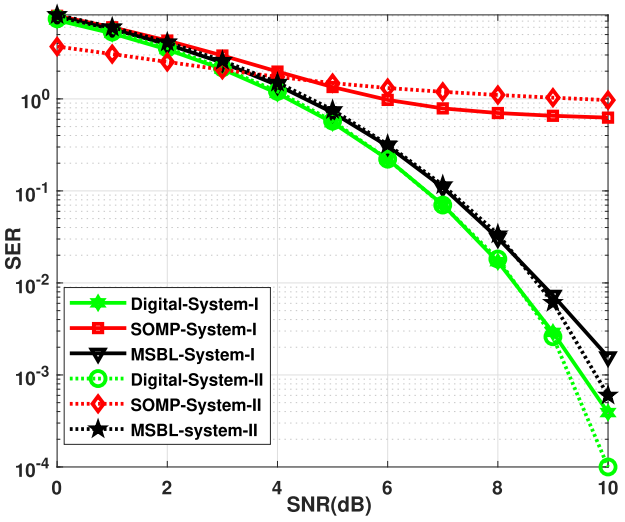

(b) Symbol error rate vs SNR in dB for the bits allocated at a fixed Signal to noise ratio $SNR = 12dB$ for frequency selective mmWave MIMO systems I and II

FIGURE 2. Transmission rate and SER performance comparison of fully-digital, SOMP and MSBL based hybrid precoder/ combiner design schemes in mmWave MIMO OFDM..

TABLE 3. Computational complexities of various steps in in each EM iteration of the proposed M-SBL algorithm.

Operation	Complex Multiplications (X)	Complex Additions (A)
E-step $\boldsymbol{\Sigma}^{(m)}$	$G_T^3 + G_T^2\,(3 + N_T)$	$2G_T^3 + G_T^2\,(N_T - 2)$
E-step $\widehat{\mathbf{F}}_{\mathrm{BB},D}^{(m)}$	$G_T^2 N_T + KG_T N_T N_s$	$G_T\,(G_T - 1)\,N_T + KG_T\,(N_T - 1)\,N_s$
M-step $\widehat{\zeta}_i^{(m)}$	$KG_T^2 N_s$	K $\mathrm{N}_s G_T$

TABLE 4. Computational complexities of multicarrier multistream integer bit allocation algorithm.

Operation	Complex Multiplications (X)	Complex Additions (A)
$b_{i,k} = \frac{P_0}{KN_s\sigma^2_{n_{i,k}}\Gamma\left[\left(\mathbf{F}^{\mathrm{M}}[k]\right)^H\left(\mathbf{F}^{\mathrm{M}}[k]\right)\right]_{i,i}}$	$N_s^2 N_T$	$N_s^2\,(N_T - 1)$

is assumed to be zero mean circularly symmetric complex Gaussian with covariance matrix $\mathbb{E}\{\mathbf{n}\mathbf{n}^H\} = \mathbf{I}_{N_R}$, where $\sigma_n^2 = 1$. In the multicarrier MSBL based precoder and combiner design approach, the hyperparameter vector is initialized as $\boldsymbol{\zeta}^{(0)} = [1\ \ 1\ \ 1\ \ \ldots\ 1]^T_{G\times 1}$ with the maximum number of EM iterations set to $M_{\max} = 150$ and the stopping parameter as $\epsilon = 10^{-9}$.

Fig. 2(a) shows the total number of bits allocated per block or per OFDM symbol for both System-I and System-II in the SNR range $0-10$ dB, averaged over 10^4 random realizations of the frequency selective mmWave MIMO channel. The SER for each input stream over each subcarrier is fixed as $\Gamma = 10^{-5}$. The simulation results show that the hybrid precoder and combiner designed using the MSBL approach is closer to that of the optimal fully-digital precoder and combiner compared to the SOMP design for both the systems. Here it is important to realize that although the SOMP leads to a higher bit allocation than the ideal transceiver, this leads to the poor SER as seen next. The SER performance corresponding to the two systems is depicted in Fig. 2(b). The SNR for evaluating the bit allocation in both the systems is set as 12dB. It can be readily observed from the results that the SER performance of the MSBL-based hybrid transceiver design is significantly lower than that of its SOMP counterpart and closer to that of the ideal fully digital design. Therefore, the simulation results in Fig. 2 comprehensively demonstrate that the MSBL approach for hybrid precoder and combiner design better approximates the optimal fully-digital precoder and combiner in each system in comparison to the SOMP algorithm. This arises due to the fact that the MSBL has improved sparse signal recovery properties in comparison to the SOMP. Furthermore, the performance of the latter scheme is highly sensitive to the choice of the dictionary matrix and stopping criterion.

Results are now described to characterize the performance of the hybrid precoder and combiner design schemes with varying number of RF chains N_{RF}. Fig. 3(a) shows the number of bits per block for System-I, for various values of the number of RF chains N_{RF}. The SNR is once again set as 12dB with the SER $\Gamma = 10^{-5}$ and the results are averaged over 10^4 random instances of the frequency selective mmWave MIMO channel. The results of a similar study are shown in Fig. 3(b) for System-II. The results demonstrate that the bits per block for the precoders and combiners designed

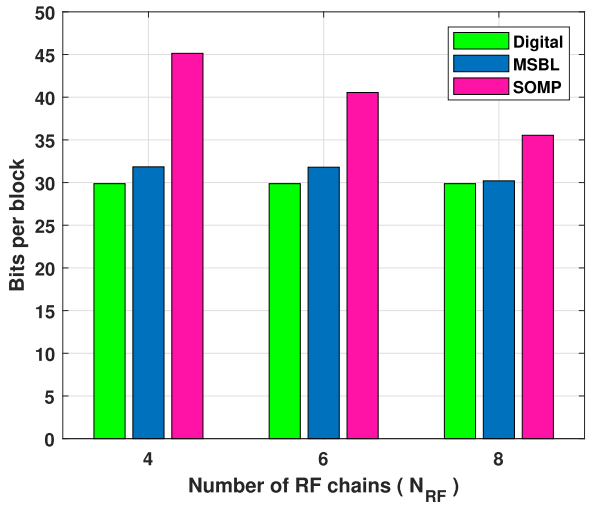

(a) Bits allocated per block vs number of RF chains (N_{RF}) at a fixed Signal to noise ratio $SNR = 12dB$, and fixed SER $\Gamma = 10^{-5}$ for frequency selective mmWave MIMO setup with $N_T = N_R = 32, G = 64, N_s = 4, L = 4, N_c = 4, K = 64$.

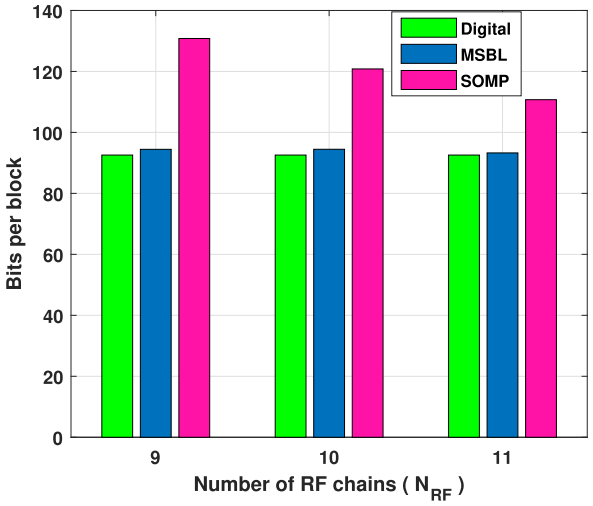

(b) Bits allocated per block vs number of RF chains (N_{RF}) at a fixed Signal to noise ratio $SNR = 12dB$, and fixed SER $\Gamma = 10^{-5}$ for frequency selective mmWave MIMO setup with $N_T = N_R = 64, G = 128, N_s = 8, L = 8, N_c = 8, K = 64$.

FIGURE 3. **Optimal bit allocation performance evaluation of hybrid precoder/ combiners with varying number of RF chains.**

using the MSBL approach is closest to that of the ideal design when compared to the SOMP algorithm for various values of the number of RF chains. Furthermore, the performance of the SOMP algorithm approaches the optimal number of bits allocated only as the number of RF chains N_{RF} increases. This can be attributed to the increased number of array steering vectors chosen from the corresponding transmit and receive array response dictionary matrices, which in turn leads to a better approximation of the ideal transceiver. On similar lines, Fig. 4(a) and Fig. 4(b) compare the resulting SER performance of hybrid precoders and combiners designed employing the MSBL and SOMP approaches for various values of the number of RF chains N_{RF}. The results once again demonstrate the improved SER performance of the former design, thus reinforcing the trend seen in previous figures.

Fig. 5(a) plots the SER performance of the proposed algorithms upon incorporating the beam squint effect, as described in [23], [24], [57], in the wideband MIMO-OFDM channel. The beam squint effect is referred to the frequency-selectivity of the array response vectors, which results in the diffusion of AoAs/ AoDs broadening the beamwidth of the desired signal in the spatial domain. To incorporate this effect, the array response vectors of Eq. (3) and Eq. (4) for the frequency f are replaced by following expressions [57]

$$\mathbf{a}_R(\theta_l^R, f) = \frac{1}{\sqrt{N_R}}\left[1, e^{-j\frac{2\pi}{\lambda}d_R\frac{f}{f_c}\cos\theta_l^R}, \ldots, e^{-j\frac{2\pi}{\lambda}(N_R-1)d_R\frac{f}{f_c}\cos\theta_l^R}\right]^T, \tag{64}$$

$$\mathbf{a}_T(\theta_l^T, f) = \frac{1}{\sqrt{N_T}}\left[1, e^{-j\frac{2\pi}{\lambda}d_T\frac{f}{f_c}\cos\theta_l^T}, \ldots, e^{-j\frac{2\pi}{\lambda}(N_T-1)d_T\frac{f}{f_c}\cos\theta_l^T}\right]^T, \tag{65}$$

where f_c is the carrier frequency. Employing this, the mmWave MIMO-OFDM CFR of the kth subcarrier can be expressed as

$$\mathbf{H}[k] = \mathbf{A}_{R,D}(\theta_R, f_k)\mathbf{D}[k]\mathbf{A}_{T,D}^H(\theta_T, f_k), \tag{66}$$

where

$$\mathbf{A}_{R,D}(\theta_R, f_k) = \left[\mathbf{a}_R\left(\theta_1^R, f_k\right), \ldots, \mathbf{a}_R\left(\theta_L^R, f_k\right)\right], \tag{67}$$

$$\mathbf{A}_{T,D}(\theta_T, f_k) = \left[\mathbf{a}_T\left(\theta_1^T, f_k\right), \ldots, \mathbf{a}_T\left(\theta_L^T, f_k\right)\right], \tag{68}$$

and $f_k \triangleq f_c + \left(k - \frac{K+1}{2}\right)\frac{B}{K}, \forall k$. It can be readily observed that the beam squint effect translates into sharing non-identical supports of the beamspace channel across the subcarriers. Fig. 5(a) plots the SER of the proposed MSBL based hybrid precoder/combiner design for two different bandwidths and number of RF chains. It can be observed that increasing the bandwidth leads to slightly poor SER owing to the dominance of the beam squint effect. However, this performance loss can be compensated via increasing the number of RF chains N_{RF}, as can be verified from the figure. Furthermore, we have also plotted the oracle LS scheme as a performance benchmark, which assumes the support of the wideband beamspace channel of the mmWave MIMO-OFDM systems to be perfectly known across all the subcarriers. The SER performance of the proposed MSBL technique with $N_{\text{RF}} = 8$ is seen to closely approach that of the Oracle LS scheme without considering the knowledge of the support of the beam space channel. This demonstrates the efficacy of the proposed MSBL scheme.

Fig. 5(b) plots the normalized approximation error $e = \frac{\|\mathbf{F}-\mathbf{F}_{\text{RF}}\mathbf{F}_{\text{BB}}\|_F^2}{\|\mathbf{F}\|_F^2}$ with respect to the number of EM iterations m. The proposed MSBL algorithm is seen to converge very fast within 20-25 EM iterations. Furthermore, the approximation

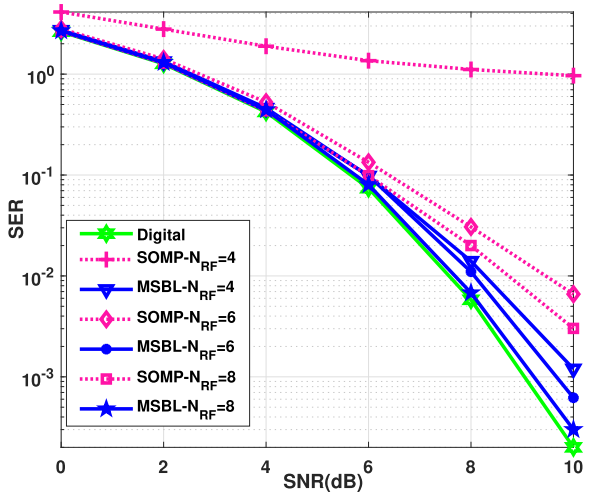

(a) Symbol Error Rate vs SNR in dB corresponding to the bits allocated at a fixed Signal to noise ratio $SNR = 12dB$ for frequency selective mmWave MIMO setup with $N_T = N_R = 32, G = 64, N_s = 4, L = 4, N_c = 4, K = 64$.

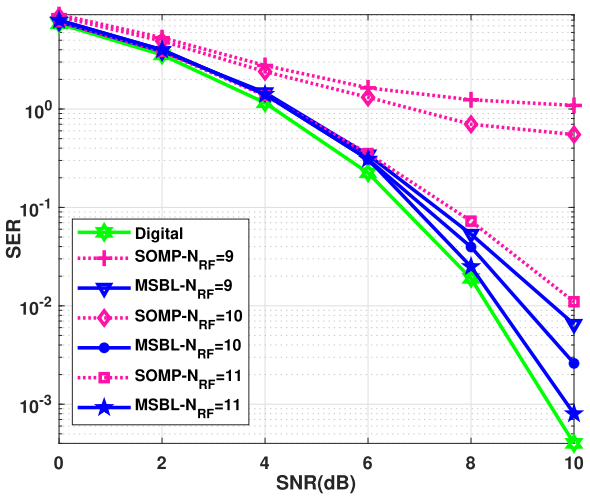

(b) Symbol Error Rate vs SNR in dB corresponding to the bits allocated at a fixed Signal to noise ratio $SNR = 12dB$, for frequency selective mmWave MIMO setup with $N_T = N_R = 64, G = 128, N_s = 8, L = 8, N_c = 8, K = 64$.

FIGURE 4. SER performance evaluation of hybrid precoder/ combiner with varying number of RF chains.

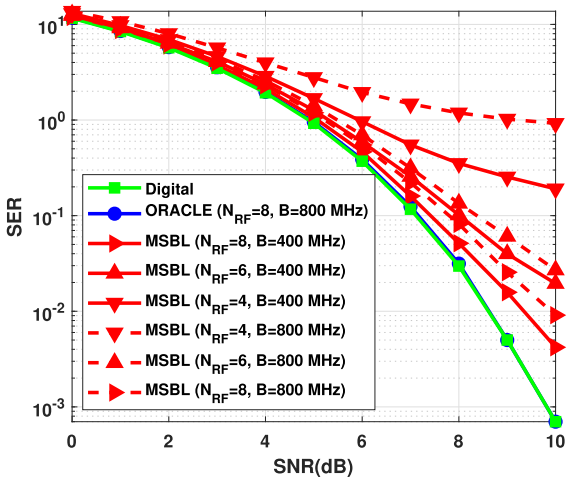

(a) Symbol error rate vs SNR in dB for the bits allocated at a fixed signal to noise ratio $SNR = 12dB$ for mmWave MIMO-OFDM systems considering the beam squint effect at $f_c = 28$ GHz.

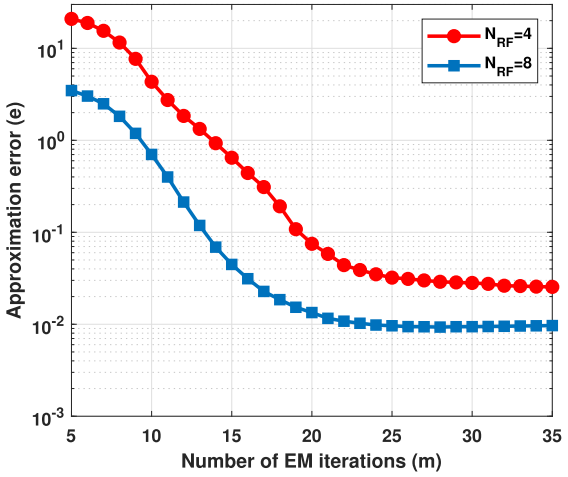

(b) MSBL convergence and accuracy in term of the approximation error $e = \frac{\|\mathbf{F}-\mathbf{F}_{\mathrm{RF}}\mathbf{F}_{\mathrm{BB}}\|_F^2}{\|\mathbf{F}\|_F^2}$ with respect to the number of EM iterations m.

FIGURE 5. Beam squint effect, and convergence versus accuracy plots.

error is seen to reduce upon increasing the number of RF chains N_{RF}.

VII. CONCLUSION

The work derived a framework for design of the optimal ideal fully-digital and hybrid precoder/combiner together with optimal bit allocation in a frequency selective mmWave MIMO-OFDM system toward transmission rate maximization with a bit error rate-based QoS constraint. This was followed by the development of more practical transceiver designs for a hybrid RF-baseband architecture that also exploits the spatially sparse scattering characteristics of the wideband mmWave MIMO channel. Toward this end, an equivalent MMV-based simultaneous sparse recovery problem was formulated to compute the hybrid precoder/combiner. Two explicit procedures were subsequently described for transceiver design, based on the simplistic SOMP approach as well as the more sophisticated MSBL technique for multiple sparse signal estimation. The proposed MSBL algorithm for the hybrid transceiver design is seen to outperform the conventional SOMP technique both in terms of SER and the required number of RF chains. The integer bit allocation algorithm optimally allocates bits across different i/p symbol streams and subcarriers to maximize the total number of bits allocated per block. Simulation results comprehensively demonstrated the performance of

the proposd schemes for a mmWave MIMO-OFDM system and also negligible performance loss of the hybrid precoder combiner architecture. The latter observation can have significant implications for practical implementation of mmWave MIMO-OFDM systems due to the lower cost and complexity associated with hybrid transceivers. Future works may extend this framework for hybrid precoder design in a wideband mmWave MIMO-OFDM system by considering the beam-squint effect as well as imperfect CSIT in both single-user and multi-user scenarios.

APPENDIX A
SOLUTION TO THE RELAXED OPTIMIZATION PROBLEM IN (14)

The KKT Conditions for the optimization problem in (15) can be stated as below

(i) Primal feasibility

$$\sum_{k=0}^{K-1} \mathrm{Tr}\left(\mathbf{F}[k]\Lambda_s[k]\mathbf{F}^H[k]\right) - P_0 \leq 0; \quad -\sigma_{s_{i,k}}^{2*} \leq 0.$$

(ii) Dual feasibility

$$\alpha^* \leq 0; \quad \beta_{i,k}^* \leq 0.$$

(iii) Complementary slackness

$$\alpha^*\left(\sum_{k=0}^{K-1}\sum_{i=0}^{N_s-1}\sigma_{s_{i,k}}^{2*}[\mathbf{F}^H[k]\mathbf{F}[k]]_{i,i} - P_o\right) = 0;$$
$$\beta_{i,k}^*\sigma_{s_{i,k}}^{2*} = 0.$$

(iv) First order condition

$$\nabla_{\sigma_{s_{i,k}}^{2*}}\mathcal{L}\left(\{\sigma_{s_{i,k}}^{2*}\}, \alpha, \{\beta_{s_{i,k}}^*\}\right) = 0.$$

In the above, $\left(\alpha^*, \beta_{s_{i,k}}^*, \sigma_{s_{i,k}}^{2*}\right)$ denote the optimal values of the Lagrangian parameters and input symbol power. From iv, we obtain

$$\sigma_{s_{i,k}}^{2*} = \frac{1}{\beta_{i,k} - \alpha[\mathbf{F}^H[k]\mathbf{F}[k]]_{i,i}}. \tag{69}$$

Using iii it follows that

$$\sigma_{s_{i,k}}^{2*} = \frac{-1}{\alpha^*\left[\mathbf{F}^H[k]\mathbf{F}[k]\right]_{i,i}}, \tag{70}$$

$$\frac{1}{\alpha^*} = \frac{-P_0}{N_s K} \tag{71}$$

Substituting (71) into (70) yields the desired result in (73).

APPENDIX B
SOLUTION TO THE EXACT OPTIMIZATION PROBLEM FOR BIT-RATE MAXIMIZATION

Without the approximation in Eq. (12), the optimization problem can be reformulated as

$$\max_{\mathbf{W}[k],\mathbf{F}[k],\sigma_{s_{i,k}}^2} b = \sum_{k=0}^{K-1}\sum_{i=0}^{N_s-1}\log_2\left(1 + \frac{\sigma_{s_{i,k}}^2}{\sigma_{n_{i,k}}^2\Gamma}\right),$$

$$\text{s.t.} \begin{cases} \sum_{k=0}^{K-1}\mathrm{Tr}\left(\mathbf{F}[k]\Lambda_{\mathbf{s}}[k]\mathbf{F}^H[k]\right) \leq P_0, \\ \mathbf{W}^H[k]\mathbf{H}[k]\mathbf{F}[k] = \mathbf{I}_{N_s}, \\ \sigma_{s_{i,k}}^2 \geq 0; k = 0, 1, \ldots, K-1; \\ i = 0, 1, \ldots, N_s - 1. \end{cases} \tag{72}$$

Upon formulating the Lagrangian for the optimization problem above, followed by the KKT framework, the optimal $\sigma_{s_{i,k}}^{2,\mathrm{new}}$ can be derived as

$$\sigma_{s_{i,k}}^{2,\mathrm{new}} = \frac{P_0}{KN_s\left[\mathbf{F}^H[k]\mathbf{F}[k]\right]_{i,i}} + \frac{\Gamma\sum_{k=0}^{K-1}\sum_{i=0}^{N_s-1}\left[\mathbf{F}^H[k]\mathbf{F}[k]\right]_{i,i}\sigma_{n_{i,k}}^2}{KN_s\left[\mathbf{F}^H[k]\mathbf{F}[k]\right]_{i,i}} - \sigma_{n_{i,k}}^2\Gamma.$$

Substituting the above value of $\sigma_{s_{i,k}}^{2\mathrm{new}}$ into the exact bit-rate expression of Eq. (11) yields

$$b_{i,k}^{\mathrm{new}} = \log_2\left(\frac{P_0}{KN_s\Gamma\left[\mathbf{F}^H[k]\mathbf{F}[k]\right]_{i,i}\sigma_{n_{i,k}}^2} + \frac{\sum_{k=0}^{K-1}\sum_{i=0}^{N_s-1}\left[\mathbf{F}^H[k]\mathbf{F}[k]\right]_{i,i}}{KN_s\left[\mathbf{F}^H[k]\mathbf{F}[k]\right]_{i,i}}\right).$$

APPENDIX C
PROOF OF LEMMA-1

The SVD of channel matrix $\mathbf{H}[k]$ associated with kth subcarrier is given as $\mathbf{H}[k] = \mathbf{U}[k]\Sigma[k]\mathbf{V}^H[k]$, whereas the ZF condition is given as $\mathbf{W}^H[k]\mathbf{H}[k]\mathbf{F}[k] = \mathbf{I}_{N_s}$. Since $\mathbf{V}[k]$ is a unitary matrix, $\mathbf{F}[k]$ can always be represented as $\mathbf{F}[k] = \mathbf{V}[k]\begin{bmatrix}\mathbf{A}[k]\\ \mathbf{A}_1[k]\end{bmatrix}$, where $\mathbf{A}[k]$ is $\rho \times N_s$ matrix and $\mathbf{A}_1[k]$ is a $(N_T - \rho) \times N_s$ matrix. Consider another precoder $\mathbf{F}'[k]$ such that it also satisfies $\mathbf{W}^H[k]\mathbf{H}[k]\mathbf{F}'[k] = \mathbf{W}^H[k]\mathbf{H}[k]\mathbf{F}[k] = \mathbf{I}_{N_s}$, and define $\mathbf{F}'[k] = \mathbf{V}[k]\begin{bmatrix}\mathbf{A}[k]\\ \mathbf{0}\end{bmatrix}$. Compare now the transmit power of $\mathbf{F}[k]$ and $\mathbf{F}'[k]$. The transmit power corresponding to $\mathbf{F}[k]$ is $\mathrm{Tr}\left(\mathbf{F}[k]\Lambda_{s[k]}\mathbf{F}^H[k]\right) = \mathrm{Tr}\left(\mathbf{A}[k]\Lambda_{s[k]}\mathbf{A}^H[k]\right) + \mathrm{Tr}\left(\mathbf{A}_1[k]\Lambda_s[k]\mathbf{A}_1^H[k]\right)$, whereas the transmit power for $\mathbf{F}'[k]$ is $\mathrm{Tr}\left(\mathbf{F}'[k]\Lambda_s[k]\mathbf{F}'^H[k]\right) = \mathrm{Tr}\left(\mathbf{A}[k]\Lambda_s[k]\mathbf{A}^H[k]\right) \leq \mathrm{Tr}\left(\mathbf{F}[k]\Lambda_s[k]\mathbf{F}^H[k]\right)$. Since the combiner matrix $\mathbf{W}[k]$ remains unchanged, both the systems have an identical subchannel noise variance. Therefore, the precoder $\mathbf{F}'[k]$ can be chosen as given in Eq. (19) without loss of generality.

APPENDIX D
PROOF OF LEMMA- 2

Consider the combiner $\mathbf{W}'^H[k]$ such that it equals the pseudo-inverse of $\mathbf{H}[k]\mathbf{F}[k]$, and $\{\mathbf{F}[k], \mathbf{W}[k]\}$ be any precoder combiner pair that satisfies the ZF condition. Let $\Delta[k] = \mathbf{W}^H[k] - \mathbf{W}'^H[k]$. Since $\{\mathbf{F}[k], \mathbf{W}[k]\}$ and $\{\mathbf{F}[k], \mathbf{W}'[k]\}$ are both ZF transceivers, we have $\Delta[k]\mathbf{H}[k]\mathbf{F}[k] = 0$. It also follows that $\Delta[k]\mathbf{W}'^H[k] = 0$. Compare now the noise variance of the ith input stream for

both the combiners $\mathbf{W}[k]$ and $\mathbf{W}'[k]$. The noise variance of the ith input stream with the combiner $\mathbf{W}[k]$ is given by $\sigma_n^2\left[\mathbf{W}^H[k]\mathbf{W}[k]\right]=\sigma_n^2\left[\left(\mathbf{W}'[k]+\Delta[k]\right)^H\left(\mathbf{W}'[k]+\Delta[k]\right)\right]$, whereas with the combiner $\mathbf{W}'[k]$, the noise variance is given as $\sigma_n^2\left[\mathbf{W}'^H[k]\mathbf{W}'[k]\right]$. Clearly,

$$\left[(\mathbf{W}'[k]+\Delta[k])^H(\mathbf{W}'[k]+\Delta[k])\right]\geq\left[\mathbf{W}'^H[k]\mathbf{W}'[k]\right]$$

. This, upon simplification, results in $\sigma_n^2\left[\Delta^H[k]\Delta[k]\right]\geq 0$. Therefore, the combiner $\mathbf{W}'^H[k]$ that has a smaller noise variance yields a higher bit-rate. Furthermore,

$$\begin{aligned}\mathbf{W}'^H[k]&=\left(\mathbf{F}^H[k]\mathbf{H}^H[k]\mathbf{H}[k]\mathbf{F}[k]\right)^{-1}\mathbf{F}^H[k]\mathbf{H}^H[k]\\&=\left(\mathbf{A}^H[k]\Lambda^2[k]\mathbf{A}[k]\right)^{-1}\left[\mathbf{A}^H[k]\ \Lambda[k]\ \mathbf{0}\right]\mathbf{U}^H[k].\end{aligned}\tag{73}$$

Hence, the noise variance for the ith input stream is given as

$$\begin{aligned}\sigma_{n_{i,k}}^2&=\sigma_n^2\left[\mathbf{W}^H[k]\mathbf{W}[k]\right]_{i,i}\\&=\sigma_n^2\left[\left(\mathbf{A}^H[k]\Lambda^2[k]\mathbf{A}[k]\right)^{-1}\right]_{i,i}.\end{aligned}\tag{74}$$

REFERENCES

[1] R. Zhang, W. Zou, Y. Wang, and M. Cui, "Hybrid precoder and combiner design for single-user mmWave MIMO systems," *IEEE Access*, vol. 7, pp. 63818–63828, 2019.
[2] A. N. Uwaechia, N. M. Mahyuddin, M. F. Ain, N. M. Abdul Latiff, and N. F. Za'bah, "On the spectral-efficiency of low-complexity and resolution hybrid precoding and combining transceivers for mmWave MIMO systems," *IEEE Access*, vol. 7, pp. 109259–109277, 2019.
[3] N. Li, Z. Wei, H. Yang, X. Zhang, and D. Yang, "Hybrid precoding for mmWave massive MIMO systems with partially connected structure," *IEEE Access*, vol. 5, pp. 15142–15151, 2017.
[4] T. S. Rappaport, R. W. Heath, Jr., R. C. Daniels, and J. N. Murdock, *Millimeter Wave Wireless Communications*. London, U.K.: Pearson, 2015.
[5] Z. Pi and F. Khan, "An introduction to millimeter-wave mobile broadband systems," *IEEE Commun. Mag.*, vol. 49, no. 6, pp. 101–107, Jun. 2011.
[6] S. Sun, T. S. Rappaport, M. Shafi, P. Tang, J. Zhang, and P. J. Smith, "Propagation models and performance evaluation for 5G millimeter-wave bands," *IEEE Trans. Veh. Technol.*, vol. 67, no. 9, pp. 8422–8439, Sep. 2018.
[7] Z. Gao, C. Hu, L. Dai, and Z. Wang, "Channel estimation for millimeter-wave massive MIMO with hybrid precoding over frequency-selective fading channels," *IEEE Commun. Lett.*, vol. 20, no. 6, pp. 1259–1262, Jun. 2016.
[8] X. Gao, L. Dai, S. Han R. W. Heath, Jr., and I. Chih-Lin, "Energy-efficient hybrid analog and digital precoding for mmWave MIMO systems with large antenna arrays," *IEEE J. Sel. Areas Commun.*, vol. 34, no. 4, pp. 998–1009, 2016.
[9] R. W. Heath, Jr., N. Gonzalez-Prelcic, S. Rangan, W. Roh, and A. M. Sayeed, "An overview of signal processing techniques for millimeter wave MIMO systems," *IEEE J. Sel. Topics Signal Process.*, vol. 10, no. 3, pp. 436–453, Apr. 2016.
[10] S. Han, C.-L. I, Z. Xu, and C. Rowell, "Large-scale antenna systems with hybrid analog and digital beamforming for millimeter wave 5G," *IEEE Commun. Mag.*, vol. 53, no. 1, pp. 186–194, Jan. 2015.
[11] W. Roh, J.-Y. Seol, J. Park, B. Lee, J. Lee, Y. Kim, J. Cho, K. Cheun, and F. Aryanfar, "Millimeter-wave beamforming as an enabling technology for 5G cellular communications: Theoretical feasibility and prototype results," *IEEE Commun. Mag.*, vol. 52, no. 2, pp. 106–113, Feb. 2014.
[12] A. Alkhateeb and R. W. Heath, Jr., "Frequency selective hybrid precoding for limited feedback millimeter wave systems," *IEEE Trans. Commun.*, vol. 64, no. 5, pp. 1801–1818, May 2016.
[13] A. Alkhateeb, O. El Ayach, G. Leus, and R. W. Heath, Jr., "Channel estimation and hybrid precoding for millimeter wave cellular systems," *IEEE J. Sel. Topics Signal Process.*, vol. 8, no. 5, pp. 831–846, Oct. 2014.
[14] O. E. Ayach, S. Rajagopal, S. Abu-Surra, Z. Pi, and R. W. Heath, Jr., "Spatially sparse precoding in millimeter wave MIMO systems," *IEEE Trans. Wireless Commun.*, vol. 13, no. 3, pp. 1499–1513, Mar. 2014.
[15] A. Alkhateeb, J. Mo, N. Gonzalez-Prelcic, and R. W. Heath, Jr., "MIMO precoding and combining solutions for millimeter-wave systems," *IEEE Commun. Mag.*, vol. 52, no. 12, pp. 122–131, Dec. 2014.
[16] J. Deng, O. Tirkkonen, and C. Studer, "MmWave multiuser MIMO precoding with fixed subarrays and quantized phase shifters," *IEEE Trans. Veh. Technol.*, vol. 68, no. 11, pp. 11132–11145, Nov. 2019.
[17] X. Qiao, Y. Zhang, M. Zhou, and L. Yang, "Alternating optimization based hybrid precoding strategies for millimeter wave MIMO systems," *IEEE Access*, vol. 8, pp. 113078–113089, 2020.
[18] S. Srivastava, A. Mishra, A. Rajoriya, A. K. Jagannatham, and G. Ascheid, "Quasi-static and time-selective channel estimation for block-sparse millimeter wave hybrid MIMO systems: Sparse Bayesian learning (SBL) based approaches," *IEEE Trans. Signal Process.*, vol. 67, no. 5, pp. 1251–1266, Mar. 2019.
[19] S. Srivastava, A. Mishra, A. K. Jagannatham, and G. Ascheid, "SBL-based hybrid precoder/combiner design for power and spectrally efficient millimeter wave MIMO systems," in *Proc. Int. Conf. Signal Process. Commun. (SPCOM)*, Jul. 2020, pp. 1–5.
[20] A. Alkhateeb, O. El Ayach, G. Leus, and R. W. Heath, Jr., "Hybrid precoding for millimeter wave cellular systems with partial channel knowledge," in *Proc. Inf. Theory Appl. Workshop (ITA)*, Feb. 2013, pp. 1–5.
[21] C.-E. Chen, "An iterative hybrid transceiver design algorithm for millimeter wave MIMO systems," *IEEE Wireless Commun. Lett.*, vol. 4, no. 3, pp. 285–288, Jun. 2015.
[22] C. Kim, T. Kim, and J.-Y. Seol, "Multi-beam transmission diversity with hybrid beamforming for MIMO-OFDM systems," in *Proc. IEEE Globecom Workshops*, Dec. 2013, pp. 61–65.
[23] H. Li, M. Li, Q. Liu, and A. L. Swindlehurst, "Dynamic hybrid beamforming with low-resolution PSs for wideband mmWave MIMO-OFDM systems," *IEEE J. Sel. Areas Commun.*, vol. 38, no. 9, pp. 2168–2181, Sep. 2020.
[24] B. Liu, W. Tan, H. Hu, and H. Zhu, "Hybrid beamforming for mmWave MIMO-OFDM system with beam squint," in *Proc. IEEE 29th Annu. Int. Symp. Pers., Indoor Mobile Radio Commun. (PIMRC)*, Sep. 2018, pp. 1422–1426.
[25] W.-L. Hung, C.-H. Chen, C.-C. Liao, C.-R. Tsai, and A.-Y. A. Wu, "Low-complexity hybrid precoding algorithm based on orthogonal beamforming codebook," in *IEEE Workshop Signal Process. Syst. (SiPS)*, Oct. 2015, pp. 1–5.
[26] H. Seleem, A. I. Sulyman, and A. Alsanie, "Hybrid precoding-beamforming design with Hadamard RF codebook for mmWave large-scale MIMO systems," *IEEE Access*, vol. 5, pp. 6813–6823, 2017.
[27] Y.-Y. Lee, C.-H. Wang, and Y.-H. Huang, "A hybrid RF/baseband precoding processor based on parallel-index-selection matrix-inversion-bypass simultaneous orthogonal matching pursuit for millimeter wave MIMO systems," *IEEE Trans. Signal Process.*, vol. 63, no. 2, pp. 305–317, Jan. 2015.
[28] C.-C. Yeh, K.-N. Hsu, and Y.-H. Huang, "A low-complexity partially updated beam tracking algorithm for mmWave MIMO systems," in *Proc. IEEE Global Conf. Signal Inf. Process. (GlobalSIP)*, Dec. 2016, pp. 748–752.
[29] M. Li, Z. Wang, X. Tian, and Q. Liu, "Joint hybrid precoder and combiner design for multi-stream transmission in mmWave MIMO systems," *IET Commun.*, vol. 11, no. 17, pp. 2596–2604, Nov. 2017.
[30] F. Dong, W. Wang, and Z. Wei, "Low-complexity hybrid precoding for multi-user mmWave systems with low-resolution phase shifters," *IEEE Trans. Veh. Technol.*, vol. 68, no. 10, pp. 9774–9784, Oct. 2019.
[31] D. P. Wipf and B. D. Rao, "Sparse Bayesian learning for basis selection," *IEEE Trans. Signal Process.*, vol. 52, no. 8, pp. 2153–2164, Aug. 2004.
[32] H. Sampath, P. Stoica, and A. Paulraj, "Generalized linear precoder and decoder design for MIMO channels using the weighted MMSE criterion," *IEEE Trans. Commun.*, vol. 49, no. 12, pp. 2198–2206, 2001.
[33] Y. Ding, T. N. Davidson, Z.-Q. Luo, and K. M. Wong, "Minimum ber block precoders for zero-forcing equalization," *IEEE Trans. Signal Process.*, vol. 51, no. 9, pp. 2410–2423, Sep. 2003.
[34] A. Scaglione, G. B. Giannakis, and S. Barbarossa, "Redundant filterbank precoders and equalizers. I. unification and optimal designs," *IEEE Trans. Signal Process.*, vol. 47, no. 7, pp. 1988–2006, Jul. 1999.

[35] C.-C. Weng, C.-Y. Chen, and P. P. Vaidyanathan, "MIMO transceivers with decision feedback and bit loading: Theory and optimization," *IEEE Trans. Signal Process.*, vol. 58, no. 3, pp. 1334–1346, Mar. 2010.
[36] A. Scaglione, P. Stoica, S. Barbarossa, G. B. Giannakis, and H. Sampath, "Optimal designs for space-time linear precoders and decoders," *IEEE Trans. Signal Process.*, vol. 50, no. 5, pp. 1051–1064, May 2002.
[37] Y.-P. Lin and S.-M. Phoong, "BER minimized OFDM systems with channel independent precoders," *IEEE Trans. Signal Process.*, vol. 51, no. 9, pp. 2369–2380, Sep. 2003.
[38] A. Yasotharan, "Multirate zero-forcing Tx-Rx design for MIMO channel under BER constraints," *IEEE Trans. Signal Process.*, vol. 54, no. 6, pp. 2288–2301, Jun. 2006.
[39] D. P. Palomar, M. A. Lagunas, and J. M. Cioffi, "Optimum linear joint transmit-receive processing for MIMO channels with QoS constraints," *IEEE Trans. Signal Process.*, vol. 52, no. 5, pp. 1179–1197, May 2004.
[40] D. P. Palomar and S. Barbarossa, "Designing MIMO communication systems: Constellation choice and linear transceiver design," *IEEE Trans. Signal Process.*, vol. 53, no. 10, pp. 3804–3818, Oct. 2005.
[41] C.-C. Li, Y.-P. Lin, S.-H. Tsai, and P. Vaidyanathan, "Optimization of transceivers with bit allocation to maximize bit rate for MIMO transmission," *IEEE Trans. Commun.*, vol. 57, no. 12, pp. 3556–3560, Dec. 2009.
[42] J. Rodriguez-Fernandez, R. Lopez-Valcarce, and N. Gonzalez-Prelcic, "Hybrid precoding and combining for frequency-selective mmWave MIMO systems with per-antenna power constraints," 2018, *arXiv:1812.02760*. [Online]. Available: http://arxiv.org/abs/1812.02760
[43] Y. Zhu, Q. Zhang, and T. Yang, "Low-complexity hybrid precoding with dynamic beam assignment in mmWave OFDM systems," *IEEE Trans. Veh. Technol.*, vol. 67, no. 4, pp. 3685–3689, Apr. 2018.
[44] C. Rusu, R. Mendez-Rial, N. Gonzalez-Prelcicy, and R. W. Heath, Jr., "Low complexity hybrid sparse precoding and combining in millimeter wave MIMO systems," in *Proc. IEEE Int. Conf. Commun. (ICC)*, Jun. 2015, pp. 1340–1345.
[45] S. Park, A. Alkhateeb, and R. W. Heath, Jr., "Dynamic subarrays for hybrid precoding in wideband mmWave MIMO systems," *IEEE Trans. Wireless Commun.*, vol. 16, no. 5, pp. 2907–2920, May 2017.
[46] Y.-S. Lin, C.-H. Hu, C.-H. Chang, and P.-C. Tsao, "One-and two-dimensional antenna arrays for microwave wireless power transfer (MWPT) systems and dual-antenna transceivers," *Int. J. Electron.*, vol. 105, no. 6, pp. 993–1010, 2018.
[47] T. A. Milligan, *Modern Antenna Design*. Hoboken, NJ, USA: Wiley, 2005.
[48] G. Dudevoir, J. Chow, S. Kasturia, and J. Cioffi, "Vector coding for T1 transmission in the ISDN digital subscriber loop," in *Proc. IEEE Int. Conf. Commun. (ICC)*, Jun. 1989, pp. 536–540.
[49] V. Friderikos, K. Papadaki, D. Wisely, and H. Aghvami, "Non-independent randomized rounding for link scheduling in wireless mesh networks," in *Proc. IEEE Veh. Technol. Conf.*, Sep. 2006, pp. 1–5.
[50] D. Zhang, A. Li, H. Chen, N. Wei, M. Ding, Y. Li, and B. Vucetic, "Beam allocation for millimeter-wave MIMO tracking systems," *IEEE Trans. Veh. Technol.*, vol. 69, no. 2, pp. 1595–1611, Feb. 2020.
[51] I. Kim, I.-S. Park, and Y. H. Lee, "Use of linear programming for dynamic subcarrier and bit allocation in multiuser OFDM," *IEEE Trans. Veh. Technol.*, vol. 55, no. 4, pp. 1195–1207, Jul. 2006.
[52] Y. T. Hou, Y. Shi, and H. D. Sherali, "Optimal spectrum sharing for multi-hop software defined radio networks," in *Proc. 26th IEEE Int. Conf. Comput. Commun.*, May 2007, pp. 1–9.
[53] D. Zhang, P. Pan, R. You, and H. Wang, "SVD-based low-complexity hybrid precoding for millimeter-wave MIMO systems," *IEEE Commun. Lett.*, vol. 22, no. 10, pp. 2176–2179, Oct. 2018.
[54] J. C. R. Horn and A. Roger, *Matrix Analysis*. Cambridge, U.K.: Cambridge Univ. Press, 1985.
[55] S. M. Kay, *Fundamentals of Statistical Signal Processing*. Upper Saddle River, NJ, USA: Prentice-Hall, 1993.
[56] C. Daskalakis, C. Tzamos, and M. Zampetakis, "Ten steps of EM suffice for mixtures of two Gaussians," 2016, *arXiv:1609.00368*. [Online]. Available: http://arxiv.org/abs/1609.00368
[57] X. Gao, L. Dai, S. Zhou, A. M. Sayeed, and L. Hanzo, "Wideband beamspace channel estimation for millimeter-wave MIMO systems relying on lens antenna arrays," *IEEE Trans. Signal Process.*, vol. 67, no. 18, pp. 4809–4824, 2019.

MANJEER MAJUMDER (Student Member, IEEE) received the B.Tech. degree in electronics and communication engineering from the RCC Institute of Information Technology, West Bengal University of Technology, India, in 2011. She is currently pursuing the M.Tech.-Ph.D. dual degree with the Department of Electrical Engineering, IIT Kanpur, India. Her research interests include channel estimation in wireless communications, MIMO, and millimeter wave communication.

HARSHIT SAXENA received the B.Tech. degree in electronics and communication engineering from Uttar Pradesh Technical University, India, in 2017. He is currently pursuing the M.Tech. degree with the Department of Electrical Engineering, IIT Kanpur, India. His research interests include applications of 5G mmWave MIMO wireless technology, and sparse signal processing.

SURAJ SRIVASTAVA (Graduate Student Member, IEEE) received the B.Tech. degree in electronics and communication engineering from Uttar Pradesh Technical University, India, in 2010, and the M.Tech. degree in communication systems from the Indian Institute of Technology (IIT) Roorkee, Roorkee, India, in 2012. He is currently pursuing the Ph.D. degree with the Department of Electrical Engineering, IIT Kanpur, Kanpur, India. From July 2012 to November 2013, he was employed as a Staff-I Systems Design Engineer with Broadcom Research India Pvt. Ltd., Bengaluru, and from November 2013 to December 2015, he was also employed as a Lead Engineer with Samsung Research India, Bengaluru, where he worked on developing layer-2 of the 3G UMTS/WCDMA/HSDPA modem. His research interests include applications of 5G mmWave MIMO wireless technology, sparse signal processing, and distributed signal processing for wireless sensor networks (WSNs) for the IoT. He awarded the Qualcomm Innovation Fellowship (QInf)-2018 from Qualcomm.

ADITYA K. JAGANNATHAM (Member, IEEE) received the bachelor's degree from the Indian Institute of Technology, Bombay, and the M.S. and Ph.D. degrees from the University of California San Diego, USA. From April 2007 to May 2009, he was employed as a Senior Wireless Systems Engineer with Qualcomm Inc., San Diego, CA, USA, where he was a part of the Qualcomm CDMA Technologies (QCT) Division. He is currently a Professor with the Electrical Engineering Department, IIT Kanpur, where he holds the Arun Kumar Chair Professorship, and is also associated with the BSNL-IITK Telecom Center of Excellence (BITCOE). His research interests include next-generation wireless cellular and WiFi networks, with special emphasis on various 5G technologies, such as massive MIMO, mmWave MIMO, FBMC, NOMA, full duplex, and others. He has been twice awarded the P.K. Kelkar Young Faculty Research Fellowship for excellence in research, the Qualcomm Innovation Fellowship (QInF), and the IIT Kanpur Excellence in Teaching Award. He awarded the CAL(IT)2 Fellowship from the University of California San Diego and the Upendra Patel Achievement Award from Qualcomm.